'La Sapienza'
University of Rome
Department of Biochemical Sciences “Rossi Fanelli”

Allosteric control of the c-di-GMP metabolism: insights from RmcA hybrid protein

Federico Mantoni
XXXI cycle
PhD PROGRAMME IN LIFE SCIENCES

Supervisor
Prof. Francesca Cutruzzolà

Tutor
Dr. Serena Rinaldo

Coordinator
Prof. Marco Tripodi

TABLE OF CONTENTS

INTRODUCTION

1.1 Bacterial Biofilm: general properties. In the environment, bacteria can live as either single organisms (planktonic mode of life) or within a multicellular community (sessile mode of life), known as biofilm. Within a biofilm, bacterial cells are stuck to each other and encapsulated in a self-produced matrix of extracellular polymeric substance (EPS) comprising polysaccharides, proteins, lipids and extracellular DNA (Jakobsen et al., 2017). Biofilm development occurs on both environmental abiotic surfaces and on biotic ones; due to this versatility to colonize different types of surfaces, biofilm formation is a critical issue in many fields including nosocomial and chronic infections (Karatan and Watnick, 2009), marine biofouling, industrial and environmental protection (Bhinu, 2005). The development of a biofilm, occurring under specific conditions, implies dramatic physiological, metabolic and phenotypic changes which are regulated by genetic, community and environmental factors. The switch from a planktonic cell to a sessile one can be divided in five different phases. After the bacterium approached closely to the surface reducing the motility (Fig. 1a), the cell may form a transient association with the surface and/or other microbes previously attached (Fig. 1b). Then the bacterium forms a stable association becoming a member of the microcolony (Fig. 1c). Biofilm-associated cells start growing and the biofilm acquires a three-dimensional architecture (Fig. 1d). Occasionally, the biofilm-associated bacteria detach from the biofilm matrix (Watnick and Kolter, 2000) becoming able to colonize a new microenvironment (Fig. 1e). Several biological factors regulate each phases of biofilm formation process: the initial interaction with the surface is promoted by force-generating structures such as type IV pili and flagella. The bacterium differentiates into a biofilm-associated cell by blocking the synthesis of factors destabilizing the biofilm, i.e. the flagellum, and by producing exopolysaccharide, fimbriae and conjugative pili reinforcing the overall biofilm structure (Watnick and Kolter, 2000). Moreover, the detachment step is dependent on changes in the environmental conditions including starvation, change in carbon source, increasing nitric oxide levels and/or iron limitations.

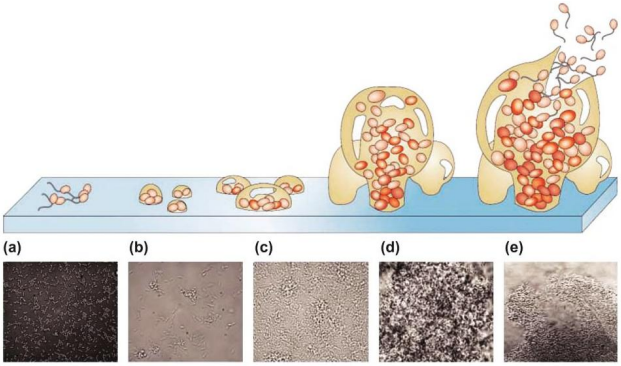

Figure 1. The main phases of bacterial biofilm development. All the illustrations of each steps (a-e) are also coupled with the equivalent photomicrograph of a biofilm of *Pseudomonas aeruginosa* (Davies, 2003).

Bacteria growing within biofilm have several advantages in comparison to the planktonic single-cell bacteria. Indeed, the biofilm formation enables bacteria to resist to predation by eukaryotes which phagocytize free-living bacteria in the environment as well as to evade immune response during human and animal infections. In addition, biofilm guarantees cooperative benefits including an increased tolerance to antimicrobials agents, longer survival period to environmental stresses as well as the ability to acquire transmissible genetic elements at accelerated rates (Tolker-Nielsen, 2014). For these reasons biofilms are particularly difficult to eliminate by the host and to eradicate with antibiotic therapy. Indeed two-thirds of bacterial infections are due to biofilms (Romling et al., 2012). Both abiotic and biological surfaces in the human body is at risk of being colonized by biofilms. For instance, indwelling devices, including urinary and intravascular catheters, prosthetic heart valves, cardiac pacemakers, and contact lenses are examples of colonized medical devices. In addition, biofilm colonize and infect biotic surfaces including nose and throat, lungs, and the gastrointestinal and urinary tracts. Infections of both abiotic and biological surfaces, often associated with hospitalization, surgical intervention, and mortality, are difficult to eradicate with traditional antibiotic strategies (Wolfmeier et al., 2017). Despite this, multi-drugs antibiotic-based therapies have been shown to be more effective than monotherapies

due to activity against multispecies biofilms (Herrmann et al., 2010). The lack of antibiotic efficacy against bacterial communities is often attributed to restricted drug accessibility within a mature biofilm. For these reasons, a deep knowledge about the molecular and biological mechanisms involved in biofilm development is required in order to develop new strategies eradicating biofilm infections. This process was often described and studied using *Pseudomonas aeruginosa*, the etiological agent of many chronic infections, as current biofilm model organism.

1.2 *Pseudomonas aeruginosa* as a model system for biofilm studies.

P. aeruginosa is Gram-negative bacterium studied as a reference model organism for biofilm research. This bacterium is often found as an environmental isolate but it can be an opportunistic pathogen involved in medical device-associated as well as chronic infections. Indeed *P. aeruginosa* plays a key role in different human biofilm infections including cystic fibrosis (CF) pneumonia, chronic bacterial prostatitis and chronic wound infections (Rybtke et al., 2015). In particular, this bacterium is the leading cause of death in CF patients. CF is a recessive genetic disease, affecting 1/2500 newborns in Europe (Moskowitz and Ernst, 2010), caused by mutation in the cystic fibrosis transmembrane conductance regulator (CFTR) gene. CFTR protein regulates the transepithelial ion flow maintaining the physiological volume of airway surface fluid: mutations in this gene lead to an accumulation of mucus inside the lower respiratory tract (Gibson et al., 2003). The accumulation of mucus makes the airways susceptible to chronic bacterial infections inducing an immune response unable to eradicate the infections, finally resulting in the respiratory failure. Despite inflammatory response and intensive antibiotic treatments, *P. aeruginosa* mediated infections are difficult to be eradicated due to its robust biofilm. Specifically, the bacterium goes through several modifications in order to survive in CF lung microenvironment including adaptation to alginate overproduction, non-motility, small-colony formation, modification of O-group chain of LPS and hypermutability (Yang et al., 2011). In addition, the stagnant mucus in the lung epithelium constitutes a nitrate-rich anaerobic environment and *P. aeruginosa* is able to produce energy under anaerobic conditions using the metabolic pathway of denitrification as well as the Arginine Deiminase (ADI) pathway (Lu et al., 2004).

Since *P. aeruginosa* patho-physiological role in CF disease is closely related to its ability to form biofilm, extending the knowledge concerning the molecular mechanisms controlling this process is crucial to develop new antimicrobial strategies.

1.3 Communication in a biofilm: Quorum sensing and Nucleotide Signalling. The two systems regulating the formation of biofilm are the Quorum Sensing (QS) and the nucleotide signalling systems (Landini, 2009). QS regulates gene expression *via* the secretion and detection of small molecules known as autoinducers (AIs) to perceive the population density. A low cell density determines a low concentration of AIs. When bacteria accumulate, forming a minimal bacterial population called quorum, the concentration of these signals increases. The detection of a threshold concentration of AIs switches the expression of genes regulating several processes such as virulence factors production, antibiotic resistance and biofilm formation (Sifri, 2008 ; Sintim et al., 2010 ; Srivastava and Waters, 2012).
The other main player in biofilm formation is represented by the nucleotide-mediated signalling (Fig. 2). Both linear as well as cyclic nucleotides act as bacterial second messengers regulating the biofilm development. One of the first nucleotide signalling molecules discovered in bacteria was the Alarmone [guanosine-(penta)tetraphosphate, (p)ppGpp] acting as the global transcriptional regulator upon amino acid starvation (Cashel and Gallant, 1969; Liu et al., 2015). Several years later, bis-(3′-5′)-cyclic diguanosine monophosphate (c-di-GMP) was firstly identified as the allosteric regulator of cellulose production by Benziman and coworkers (Ross et al., 1987), but only in the last 20 years the role of c-di-GMP as the main bacterial second messenger has been emerged. Among the Cyclic Dinucleotide (CDN) signalling field there are two other signalling molecules: cyclic di-AMP (c-di-AMP) and cGMP–AMP (cGAMP). The c-di-AMP signalling network is involved in several cellular functions including DNA integrity, potassium homeostasis, gene expression, biofilm formation and sporulation process in *Bacillus subtilis* (Jenal et al., 2017). cGAMP metabolism is very intriguing because it is produced by both bacteria and metazoans. Bacterial cGAMP has a 3′-3′ linkage and was originally discovered in *Vibrio cholerae* as a signalling molecule required for host colonization (Kato et al., 2015).

Furthermore, numerous recent studies have demonstrated that cyclic dinucleotides are potent immunostimulatory compounds since they can activate the STING (STimulator of INterferon Genes) signalling pathway (Karaolis et al., 2007 ; Chen et al., 2010 ; Jenal et al., 2017).

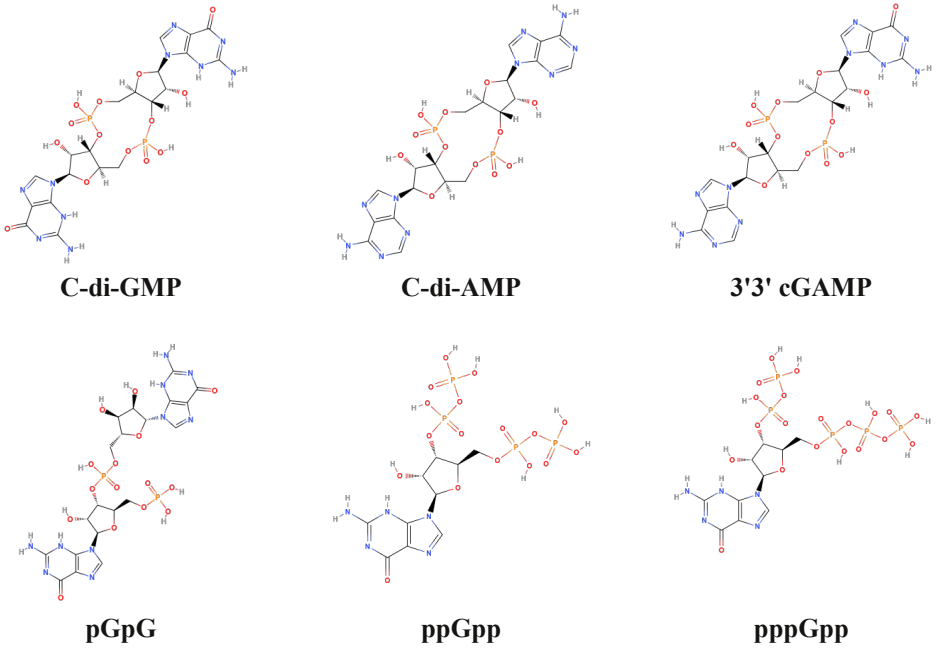

Figure 2. Chemical structures of the main bacterial second messengers

1.4 Cyclic di-GMP metabolism. Cyclic di-GMP, discovered as an allosteric factor required for activation of cellulose biosynthesis in *Gluconacetobacter xylinus* (Ross et al., 1987), is the most abundant bacterial second messenger. In the last 20 years, the importance of c-di-GMP in the bacterial physiology raised up. Indeed, the second messenger regulates many phenotypes including cell differentiation in *Caulobacter crescentus*, the heterocyst formation in cyanobacteria, development and antibiotic production in streptomycetes, long-term nutritional stress survival, lipid metabolism and transport in mycobacteria (Römling et al., 2013).

C-di-GMP is considered the intracellular signaling molecule regulating the biofilm formation and dispersal in several bacteria species, including *Salmonella enterica*, *Escherichia coli*, *G. xylinus*, *V. cholerae* and *P. aeruginosa*. A general principle is that high c-di-GMP levels are associated to biofilm formation while low levels promote biofilm dispersal (Antoniniani et al., 2013). However some exceptions of this general mechanism are now emerging. As an example, *P. aeruginosa* biofilms are estimated to contain on average 75–110 pmol of c-di-GMP per mg of total cell extract, while planktonic cells are appraised to contain less than 30 pmol/mg (Basu Roy and Sauer, 2014).

C-di-GMP regulates biofilm formation by producing extracellular matrix components such as: exopolysaccharides, adhesive pili, curli fimbriae, adhesins as well as extracellular DNA (Römling et al., 2012). Indeed c-di-GMP is able to control biofilm-related targets at different levels including the transcriptional, post-transcriptional and post-translational ones. Concerning the mechanism of c-di-GMP mediated control of biofilm formation, the scenario is very complex. The c-di-GMP molecule is characterized by an high degree of polymorphism which favours its interaction with a large number of proteins and nucleic acids using different binding modes (Fig. 3). In solution, c-di-GMP can exist in the monomeric, dimeric, tetrameric and octameric form depending on its concentration and the presence of metal ions. However, under physiological conditions, the main aggregation states are a monomer in equilibrium with the intercalated dimer; both forms were observed in crystal structures of c-di-GMP binding and metabolizing proteins (Chan et al., 2004; Tchigvintsev et a., 2010; Shu et al., 2012) (Fig. 3).

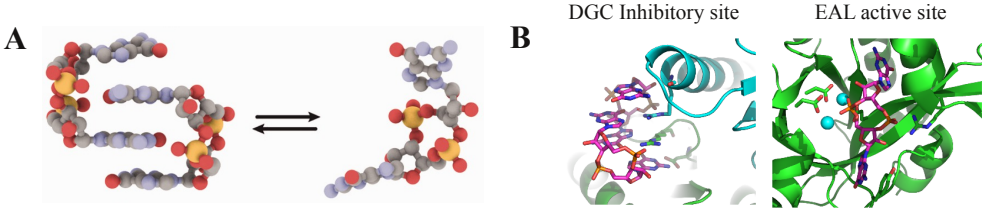

Figure 3. Polymorphism of c-di-GMP molecule. (A) 3D structure of monomeric and dimeric c-di-GMP. The equilibrium in solution between these two species is influenced by the presence of monovalent or divalent cations (Stelitano et al., 2013). (B) Heterogeneity of c-di-GMP binding to proteins. C-di-GMP binds as intercalated dimer to the inhibitory site of DGC (left panel ; PDB 2V0N), while as a monomer to the active site of EAL PDE (right panel ; PDB 4LJ3).

The monomer-dimer equilibrium likely plays a physiological role, allowing bacteria to sense and to control different local c-di-GMP concentrations.

The intracellular levels of c-di-GMP are controlled by the rate of its synthesis and degradation which are bidirectionally regulated by diguanylate cyclases (DGCs) and phosphodiesterases (PDEs), respectively. The first group of enzymes produces c-di-GMP and they are characterized by the structurally conserved domain GGDEF, named from the strictly conserved signature (Gly-Gly-Asp-Glu-Phe) at the active site. On the other hand, PDEs enzymes are divided in two groups: the first group of enzymes, characterized by the consensus sequence EAL (Glu-Ala-Leu) responsible for the hydrolytic activity, hydrolyses c-di-GMP to the linear dinucleotide pGpG; the other group of PDEs named HD-GYP proteins (His-Asp and Gly-Tyr-Pro) hydrolyses c-di-GMP directly to GMP. The distribution of c-di-GMP metabolizing proteins among species of the same phylum is not homogenous: free living bacteria with different environmental lifestyles carry more genes coding for putative c-di-GMP metabolizing enzymes than obligate parasites (Galperin, 2005). Interestingly, genomic database contains sequences of GGDEF and EAL domain proteins encoded by plants and lower eukaryotes. While the function of plant GGDEF and EAL domain proteins remains unknown, in the lower eukaryotes the c-di-GMP acts as a developmental regulator (Chen and Schaap, 2012). The genome of *P. aeruginosa* PAO1 encodes for 42 proteins likely involved in c-di-GMP metabolism, in particular 18 GGDEF containing DGCs, 5 EAL containing PDEs, 16 GGDEF/EAL hybrid proteins, and 3 HD-GYP containing PDEs. In addition most of these proteins often carry various sensory domains on their N-terminus, likely participating in transduction of environmental stimuli, being c-di-GMP levels finely controlled by different environmental settings (Ha and O'Toole, 2015). The first data suggesting that c-di-GMP metabolism was a component of the cellular signal transduction network derived from the presence of the GGDEF and EAL domains in tandem with the oxygen-sensing PAS (Per-ARNT-Sim) sensory domain in DGCs and PDE of *G. xylinus* (Chang et al., 2001). This discovery suggested a possible modulation of enzymatic activity of the two domains by the upstream sensory one(s).

In particular these domains allow the proteins to perceive several signals such as: nutrients (Paiardini et al., 2018), gases (O_2, NO and CO) (Cutruzzolà and Frankenberg-Dinkel, 2016), the redox state (Qi et al., 2009), light, quorum-sensing molecules and many other signals (Henry and Crosson, 2011 ; Deng et al., 2012). In addition, these c-di-GMP metabolizing proteins are often part of Two Components System network since they can bear REC domain, modulating c-di-GMP levels in response to signals received by their cognate sensor His kinases (Galperin, 2010). Among the players involved in c-di-GMP network, the c-di-GMP receptors represent an heterogeneus group of proteins. Indeed, the detection of c-di-GMP levels within the cell and the resulting activation of a specific cellular signaling pathway is mediated by both c-di-GMP effectors and receptors. In particular, c-di-GMP effectors are proteins whose activity allosterically changes upon c-di-GMP binding. This event induces effectors to undergo conformational changes, transcriptional activation or repression, protein-protein interactions and enhanced enzymatic activity. On the other hand, c-di-GMP receptors activate specific signalling pathways after the c-di-GMP binding (Valentini and Filloux, 2016). Both c-di-GMP receptors and effectors are able to interact with c-di-GMP through different domains. Due to the absence of a common domain involved in c-di-GMP recognition, the bioinformatic identification of proteins able to bind c-di-GMP proved to be challenging. Since c-di-GMP can adopt different conformations, it can interact with RNAs, as well as different classes of proteins (Römling et al., 2013). Indeed, c-di-GMP receptors include riboswitches, transcription factors, PilZ domain receptors, I-site receptors and inactive EAL/HD-GYP domain receptors. Riboswitches are located in the 5' untranslated regions of mRNAs (5'-UTR) showing different conformations depending on c-di-GMP binding, which can promote or inhibit transcriptional termination and translation (Hengge, 2016). Among the c-di-GMP protein receptors, PilZ containing proteins are the most studied. PilZ domain binds both monomers and dimers of c-di-GMP coupling the sensing of c-di-GMP to several processes. Moreover degenerate catalytically inactive GGDEF and EAL domains bind to c-di-GMP acting as receptors. For instance, GGDEF containing protein PopA from *C. crescentus* binds c-di-GMP regulating cell cycle (Duerig et al., 2009) as well as the inactive EAL containing protein LapD from *Pseudomonas fluorescens* acts as a c-di-GMP receptor

promoting the biofilm formation (Dahlstrom et al., 2015). The c-di-GMP network properties, including different binding modes, multidomain metabolizing enzymes and heterogeneous receptors (Fig. 4), suggest that c-di-GMP based physiological responses are extremely sophisticated, making bacteria able to react to several environmental conditions. Due to the high complexity of the c-di-GMP network, the molecular details of c-di-GMP signalling are still fragmentary and few biochemical and molecular data on proteins involved in c-di-GMP turnover are available (Romling et al., 2013). A brief summary of so far available functional and structural data of c-di-GMP enzymes is given below.

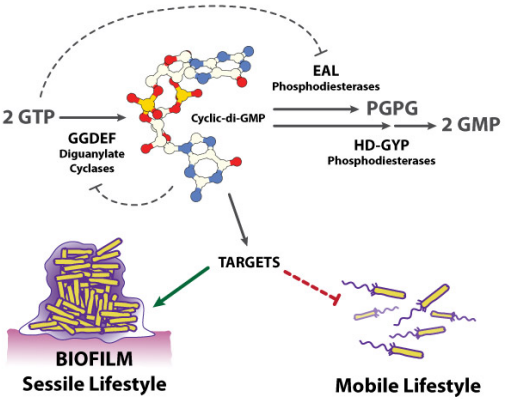

Figure 4. Main components of c-di-GMP metabolic and signalling network

1.4.1 Diguanylate Cyclases: the makers. The GGDEF domain was originally described in 1995 by Hecht and Newton in the response regulator PleD from *C. crescentus* (Hecht and Newton, 1995). PleD is a multidomain DGC characterized by a REC1-REC2-GGDEF domain organization where the upstream receiver domains regulate the downstream GGDEF activity. Structural and mechanistic studies on PleD proposed insights about the modes of substrate binding, catalysis, enzyme activation and inhibition (Chan et al., 2004 ; Wassmann et al., 2007). The c-di-GMP formation is a two-step reaction requiring two molecules of GTP and resulting in two molecules of pyrophosphate as reaction by-products. Two Mg^{2+} or Mn^{2+} cations are required for phosphoester bond formation as well as the two GTP molecules

aligned in an antiparallel orientation. GGDEF domains function as homodimers where both monomers contribute to the formation of the active site. The active site, or A site, of the GGDEF domain is crucial for GTP binding. The GG(D/E)EF signature forms an hairpin where the first two Gly and the third amino acid are needed for catalysis and the Asp/Glu plays an additional role in metal coordination while the forth Glu residue is the main amino acid involved in metal ion coordination. Finally, the Phe residue plays a structural role, keeping the hairpin in the position. The enzymatic regulation of this class of proteins is mediated by two different mechanisms. The first mechanism requires conformational dimerization of the GGDEF domains in response to changes in the sensory domains linked to the GGDEF domains Indeed, the GGDEF dimerization process takes place after the REC domain are phosphorylated through one of its cognate kinases (Paul et al., 2004). Since the dimerization increases the enzymatic activity in comparison with monomeric form of PleD, this implies that the phosphorylation-mediated dimerization represents the main mechanism controlling PleD diguanylate cyclase (Fig. 5 ; Paul et al., 2007).

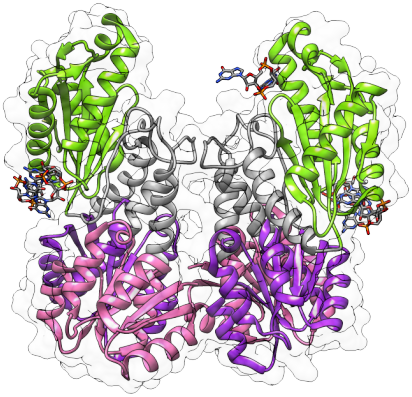

Protein	**C-di-GMP (nmol min^{-1} mg^{-1})**
PleD	3.32±(0.7)
PleD (after dimerization)	159.97±(22.6)

Figure 5. PleD diguanylate cyclase. The quaternary structure of PleD with c-di-GMP bound is reported on the left (the GGDEF domain is labeled in green while the REC1 and REC2 are labeled in purple and pink, respectively). Once REC1 is phosphorilated, the dimerization process occurs, increasing the rate of the enzyme, as indicated in the table on the right.

A further mechanism regulating the activation/inactivation of DGCs is based on a feedback inhibition. The I-site, if present, is a functional motif comprising four residues (RXXD where 'X' is any residue) located five amino acids upstream of the GGDEF signature. C-di-GMP binds as an intercalated dimer to the I-site (Fig. 3B, left panel) inducing an interlock between two either identical (i.e. GGDEF/GGDEF) or different domains (i.e. GGDEF/REC, GGDEF/GAF, YcgR-N/PilZ). The c-di-GMP binding to the I-site blocks the GGDEF movement required for the homodimerization rearrangement thus hampering the catalytic activity. In PleD, the binding of c-di-GMP to I-site induces structural rearrangements of GGDEF altering kinetic parameters. Since each domain provides one of the two key arginines, in the case of the I-site of DGCs the first arginine is provided by the primary I-site (Ip) of the GGDEF domain (the conserved RxxD motif), while the second may be recruited from the secondary I-site (Is) of another GGDEF domain or from a different one. The c-di-GMP mediated feedback inhibition is the best understood example of the allosteric regulation mediated by this second messenger.
An exception of this allosteric regulation is represented by YfiN from *P. aeruginosa*. Despite the presence of a primary I-site, this protein does not undergo to a feedback inhibition since it lacks of the additional secondary site required for I-site-dependent feedback regulation. In this case, protein activation leading to the two GGDEF to be faced requires the upstream HAMP domains transducing a periplasmic signal (Giardina et al., 2013).

1.4.2 Phosphodiesterases: the breakers. A first general characterization of an EAL-containing phosphodiesterases was performed by Benzimann and collegues in 1987 (Ross et al., 1987). This domain hydrolyzes c-di-GMP into linear 5'-pGpG which is then degraded by different enzymes. The majority of EAL-containing PDEs form dimers and this quaternary structure is critical for protein activation by cellular and environmental stimuli. The dimerization interface is evolutionarily conserved and it is formed by two helices and a long loop. Specifically, the α5 helix is directly connected through loop 6 to two central Asp residues coordinating the metal ions in the active site (Barends et al., 2009). This loop undergoes several structural rearrangements and it can act as an hinge coupling the EAL conformation to catalytic activity through the repositioning of metal ions within the active site.

Based on structural characterization of an EAL-containing PDE, several clues about the c-di-GMP binding site and catalytic mechanism were obtained (Sundriyal et al., 2014). EAL activity requires either Mn^{2+} or Mg^{2+} while it is inhibited by Ca^{2+}: EAL domain binds c-di-GMP monomer through two metal cations which are also involved in coordination of two water molecules. One of this water molecules is required for the hydrolytic attack on a phosphoester bond of the c-di-GMP. A higher pH and the presence of Mn^{2+}/Mg^{2+} promote the optimal bond lengths in the metal-water cluster while Ca^{2+} distorts the distances inside the cluster resulting in an inhibitory effect. Concerning the catalytic mechanism, the Glu residue within the EAL motif is crucial for PDE activity: indeed, this residue is involved in coordination of one of the metals inside the active side (Fig. 3B right panel). In *P. aeruginosa*, the first EAL-containing PDE identified was RocR (Fig. 6), component of the RocSAR signalling system.

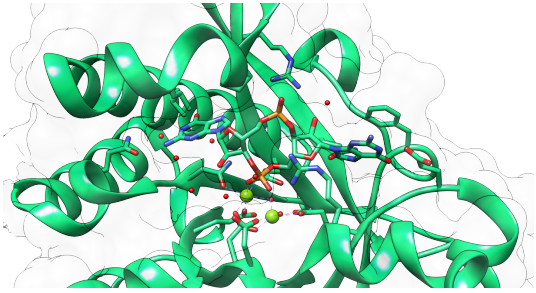

Protein	**K_M (µM)**	**k_{cat} (min^{-1})**
RocR	3.2±0.3	0.67±0.03

Figure 6. The EAL active site of RocR. The binding of the substrate requires the presence of two cations (green spheres) involved in the coordination of water molecules. One water molecule is involved in the hydrolytic attack on a phosphoester bond of the c-di-GMP.

This system, controlling the biofilm formation and virulence genes expression, is composed of a membrane sensor RocS1 and two response regulators, RocA1 and RocR. RocR activity is triggered by phosphorylation and the protein competes with RocA1 for the phosphoryl transfer from the RocS1 sensor (Kulasekara et a., 2005). The degradation of the pGpG produced by EAL containing enzymes is mediated by different proteins. Specifically, the oligoribonuclease Orn, which hydrolyses nanoRNAs (2–5 nucleotides in length), is the main enzyme able to degrade pGpG (Orr et al., 2015).

In addition, other enzymes are involved in the degradation of pGpG, including few EAL PDE such as RbdA, which shows pGpG hydrolytic activity, named PDE-b activity, and the second family of phosphodiesterases characterized by the HD-GYP catalytic domain. In contrast to EAL-containing enzymes able to convert c-di-GMP into the linear product pGpG, HD-GYP domain hydrolyses c-di-GMP producing two molecules of GMP and this catalytic activity requires divalent cations, most likely Mg^{2+} or Mn^{2+}. This class of phosphodiesterase is not ubiquitous in bacteria (Galperin, 2005). Bd1817, from *Bdellovibrio bacteriovorus*, is an unconventional HD-GYP protein, lacking the active-site tyrosine present in the HD-GYP family members, whose crystallographic structure revealed the fold of the HD-GYP domain, together with some important clues about the catalytic and the regulation mechanisms (Lovering et al., 2011). This enzyme shows a binuclear iron center into the active site and sequence alignment revealed that the residues around this metal center are structurally conserved also in the conventional HD-GYP proteins. Despite this, the first structure of an active HD-GYP domain containing PDE indicated that a trinuclear iron-binding site is required for its catalysis (Bellini et al., 2013). In addition the active site is different from that observed in the EAL enzymes, since the limited access to the active-site cleft suggests a different mechanism of activity regulation. The genome of *P. aeruginosa* encodes for three HD-GYP containing-proteins, PA4108, PA4781 and PA2572. Few *in vivo* and *in vitro* data describing these enzymes are available. For instance, biochemical and structural data concerning PA4781 showed that this enzymes has a bi-metallic active site, hydrolyses c-di-GMP to GMP *in vitro* through a two-step reaction via the linear intermediate pGpG, and this reaction is regulated upon the phosphorylation of the upstream REC domain. Interestingly, this protein is able to degrade pGpG to GMP and, moreover, PA4781 preferentially binds to pGpG over c-di-GMP, indicating that both this protein may work as an unconventional HD-GYP phosphodiesterase and that pGpG could act as a signalling molecule (Stelitano et al., 2013 ; Rinaldo et al., 2015).

1.4.3 Hybrid Proteins: the enzymatic conundrum. Genomic analysis revealed that around 1/3 of all GGDEF domains and approximately 2/3 of all EAL domains are found on the same polypeptide chain (Seshasayee et al., 2010). The existence of hybrid proteins bearing both antagonistic catalytic domains implies an enzymatic riddle regarding the final catalytic output. For this reason, the study of hybrid proteins is really challenging. Two possibilities may explain the enzymatic conundrum of hybrid proteins. One scenario is that both domains are enzymatically active but they are differentially regulated by environmental and/or cellular signals resulting in one prevalent activity. This first hypothesis is supported by MorA, the first bifunctional hybrid protein characterized (Phippen et al., 2014) and MucR (Hay et al., 2009) from *P. aeruginosa*. MorA is a dimeric membrane protein with PAS sensory domains in the cytosolic portion which is followed by downstream GGDEF and EAL domains. MorA shows both diguanylate cyclase and phosphodiesterase activities and, in particular, the PDE activity is regulated by the GGDEF domain by increasing the turnover rate of the enzyme (Fig. 8). The other example of hybrid protein showing both DGC and PDE activities which are differently regulated is MucR.

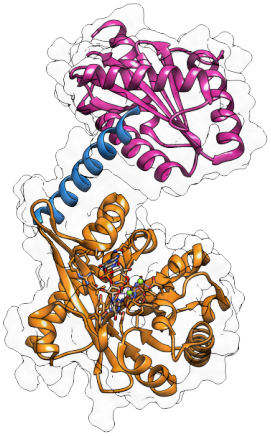

Protein	PDE turnover (%)
MorA (GGDEF-EAL)	100 ± 8.8
MorA (EAL)	14 ± 1.4

Figure 8. Monomer of MorA hybrid protein from *P. aeruginosa*. MorA bound c-di-GMP within the active site of EAL domain (orange). The catalysis is regulated by the GGDEF domain (purple) increasing the turnover rate of the enzyme (Phippen et al., 2014)

The GGDEF and the EAL domains of MucR are activated in different growth phases: in planktonic cells, MucR DGC activity positively regulates alginate biosynthesis while in biofilms, it functions as a PDE regulating the dispersal upon the nitric oxide or glutamate exposure (Hay et al., 2009 ; Wang et al., 2015). The other scenario is represented by hybrid proteins showing either one or both GGDEF-EAL inactive domains which are still able to recognize the substrates as a signal; signal recognition triggers an allosteric response such as conformational changes or protein-protein interactions. In agreement with this possibility, there is the example of the hybrid protein LapD from *P. fluorescens*. LapD is an inner-membrane protein required for biofilm formation and maintenance. This protein has degenerate and inactive GGDEF and EAL domains: the protein can bind c-di-GMP but cannot synthesize or degrade it. When c-di-GMP is absent, LapD shows an autoinhibited conformation where the upstream HAMP domain and the GGDEF domain block c-di-GMP from accessing the EAL domain. In this autoinhibited state, the periplasmic domain of LapD is involved in an uncompetent binding state with the cysteine protease LapG. This interaction allows LapG to cleave LapA from the cell surface preventing the biofilm formation early steps. Upon an increase in cytoplasmic c-di-GMP, a large conformational change at the level of the GGDEF and HAMP domains takes place, allowing the EAL domain dimerization. This signal is transmitted to the periplasm where LapD interacts with LapG in a competent way. After this protein-protein interaction, LapG is no longer able to cleave LapA from the cell surface, resulting in biofilm formation by the activation of different proteins involved in stable surface attachment (Newell et al., 2009 ; Navarro et al. 2011).

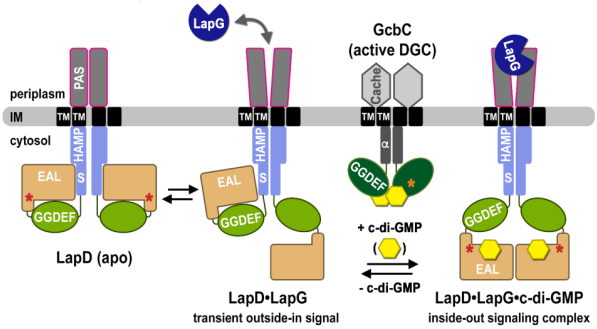

Figure 9. C-di-GMP-dependent regulation of the periplasmic protease LapG via the inner membrane protein LapD. Conformational changes expose a periplasmic binding site for LapG on LapD periplasmic PAS domain. In addition, c-di-GMP to the inactive EAL domain of LapD increases ~6 fold the apparent affinity for LapD, sequestering the protease away from its substrates, the adhesin proteins LapA in *P. fluorescens* (Cooley et al., 2016).

Another example of protein belonging to this last group is the hybrid protein CC3396 from *C. crescentus*. CC3396 shows only the EAL-dependent phosphodiesterase activity while the GGDEF domain lacks enzymatic activity. Interestingly, the GGDEF domain is able to bind GTP within the A-site and this binding triggers PDE activation by lowering the K_M for c-di-GMP of EAL domain (Christen et al., 2005), suggesting that the GGDEF domain is involved in an allosteric regulation of the EAL catalytic activity via GTP molecule.
Despite the relevance of these proteins considering their involvement in pathogenic settings and the intriguing allosteric control of their activity, few mechanistic data are available in the literature.

1.5 The regulation of c-di-GMP signalling. The extraordinary large number of proteins involved in c-di-GMP network in many bacterial species suggests that c-di-GMP signalling network is complex. Indeed, these networks include enzymes, receptors and effectors which are able to sense and respond to both cellular and environmental cues, adjusting the c-di-GMP levels in order to control a specific phenotypic output. All these observations lead to an open question: how is a bacterial cell able to coordinate several proteins involved in c-di-GMP metabolism and signalling?

To solve this issue, several models have been proposed to explain how c-di-GMP signalling networks control specific effector proteins at the right time or location within the bacterial cell. One model, called 'Affinity Model', depends on binding affinity of different effectors to c-di-GMP. In *P. aeruginosa* affinity differences greater than 140-fold among its eight PilZ domain-containing proteins were found (Christen et al., 2010; Pultz et al., 2012). According to this affinity model, global pools of c-di-GMP modify expression and activity of c-di-GMP-metabolizing enzymes (Krasteva et al., 2010 ; Hickman et al., 2008). Frequent observations showing that genetic deletion of a particular DGC or PDE can lead to a specific phenotype despite the apparent redundancy of DGCs and PDEs in single species has reinforced the hypothesis about a ‘local signalling’ of c-di-GMP based on spatial distributions of c-di-GMP metabolizing proteins. This hypothesis implies the presence of protein-protein interactions among DGCs, PDEs, and effectors, spatially close to each other, allowing local signaling. Consistent with this 'Local Model', different *in vivo* evidences have been found in several bacterial species including *Yersinia pestis*, *E. coli* and *P. fluorescens* (Bobrov et al., 2008 ; Lindenberg et al., 2013 ; Dahlstrom et al., 2015). Regardless the signalling model proposed, the c-di-GMP network, controlling several cellular functions, is regulated at multiple levels: allosteric regulation of an enzyme activity or protein function, regulation of gene expression *via* the modulation of a transcription factor and as well as *via* direct interaction with noncoding RNA molecules, i.e. riboswitches. As described above, the c-di-GMP metabolizing enzymes can be subjected to an allosteric regulation mediated by a plethora of mechanisms and small molecules (Chan et al., 2004 ; Wassmann et al., 2007 ; Newell et al., 2009 ; Navarro et al. 2011 ; Christen et al., 2005). In addition, the c-di-GMP signalling has a key role in transcriptional regulation of genes involved in biofilm development and dispersal. An example of transcriptional circuit affected by c-di-GMP is represented by the transcriptional factor BrlR from *P. aeruginosa*. BrlR is an Helix-Turn-Helix (HTH) transcriptional factor belonging to the MerR family of multidrug transport activators which contributes to the drug tolerance of *P. aeruginosa* biofilms. This protein is able to bind its own promoter regulating its expression. Interestingly the BrlR-DNA interaction is enhanced upon the c-di-GMP binding, contributing to *brlR* expression (Chambers et al., 2014) which, in turn, promotes multidrug resistance in biofilm.

C-di-GMP signalling is also involved in regulation of the protein translation through small non-coding RNAs called riboswitches. Riboswitches are a 5′ UTR elements of bacterial mRNAs and consists of two different modules: the aptamer and the expression domains. The aptamer module binds different ligands triggering a conformational change on the expression domain that directly modulate the translation of the downstream open reading frame (ORF). In *V. cholerae*, the Vc2 c-di-GMP riboswitch has two possible secondary structures: a ligand-bound state which blocks the initiation of translational and a free ligand state which activates translational beginning. Upon c-di-GMP binding to aptamer module, the Vc2 riboswitch secondary structure undergoes to a conformational change masking of Ribosome Binding Sequence (RBS) (Inuzuka et al., 2018).

1.6 The role of nutrients on c-di-GMP signalling and metabolism. In addition to these regulatory strategies, c-di-GMP metabolizing enzymes are controlled by environmental cues including nutrients levels. In *P. fluorescens*, several groups of genes are regulated under different nutrient conditions, suggesting that the the nutrient-dependent regulation may be an efficient method to control the c-di-GMP network by controlling single proteins under specific environmental conditions (Dahlstrom et al., 2018). However, little is known about how nutrients involved in biofilm development are perceived and how signaling pathways translate these cues into the modulation c-di-GMP levels. It has been established that the switch between a free living cell to a sessile one occurs as a response to the availability of nutrients. Indeed, nutrient-depleted environments favour the biofilm formation while the biofilm dispersion occurs in response to a change in the nutrient composition. In particular, it has been demonstrated that the availability of nutrients at high concentration represses the formation of biofilms favouring the detachment (Rochex and Lebeault, 2007). All these observations suggested that bacteria perceive the availability of nutrients in the environment through a variety of complex regulatory networks likely regulating the c-di-GMP metabolism in a nutrient-dependent way (Sauer et al., 2004). Despite the well established link between nutrients availability and biofilm development, few molecular data are available concerning both the expression of c-di-GMP related genes as well as the regulation of c-di-GMP metabolizing enzymes in response to nutrients.

For instance, transcription of the *rapA* gene, encoding for a hybrid protein of *P. fluorescens* showing only PDE activity, has been demonstrated to be upregulated when cells are grown in a low phosphate medium (Monds et al., 2007). Another few examples of the role of nutrients as regulators of c-di-GMP signalling were described in *V. cholerae*. When the bacterium reaches the stomach, during its infectious process , the exposure to bile acids induces the activation of three DGCs, CdgH, VC1372, and CdgM, leading to an increase of c-di-GMP concentration (Conner et al., 2017). Moreover, polyamines, within the human gastrointestinal tract, represent another environmental signal involved in c-di-GMP metabolism in *V. cholerae*. Norspermidine and spermidine regulate in an opposite way biofilm formation controlling the membrane-bound phosphodiesterase MbaA and its periplasmic partner NspS. Norspermidine binds to NspS which interacts with the periplasmic portion of MbaA blocking its PDE activity. This signalling pathway triggers biofilm formation. On the other hand, spermidine blocks biofilm development and this repression occurs via competition with norspermidine for NspS binding site (Goforth et al., 2013). In *P. aeruginosa*, glutamate plays a role in biofilm dispersal modulating c-di-GMP levels. This metabolite is at the crossroad between anabolism and catabolism, playing a role in cell division during amino acid starvation via ppGpp (Sperber and Herman, 2017). NicD is a transmembrane GGDEF diguanylate cyclase participating in a complex signaling mechanism. This diguanylate cyclase is activated upon the binding of glutamate and this event triggers a signalling cascade resulting in the activation of the phosphodiesterase DipA, which reduces c-di-GMP levels (Basu Roy et al., 2014). In addition to glutamate, arginine has a crucial role in *P. aeruginosa* metabolism. This bacterium is able to use this amino acid as source of carbon, energy and nitrogen, via a complex metabolic network (Fig. 10). This amino acid can be catabolized by arginine deiminase (ADI) producing ATP under low oxygen tension and this enzyme is inducible by exogenous L-arginine (Lu etal., 2004). Moreover, environmental L-arginine plays a key role in chronic infections, virulence and antibiotic resistance in *P. aeruginosa* biofilm (Schreiber et al., 2006; Son et al., 2007; Barbier et al., 2014; Peng et al., 2017).

At molecular level, extracellular L-arginine controls the production of phenazines (Ha et al., 2011) which in turn modulates biofilm formation through the second messenger c-di-GMP (Okegbe et al., 2017). Despite the presence of L-arginine sensory systems involved in the regulation of c-di-GMP levels have been proposed (Mills et al., 2015; Romling et al., 2015), little is known about the genes involved in these signalling pathways in *P. aeruginosa* (Rinaldo et al., 2018).
These few examples clearly underline that different nutrients, energy source and environmental conditions have strong effects on biofilm development and homeostasis, controlling at different levels the c-di-GMP signalling network.

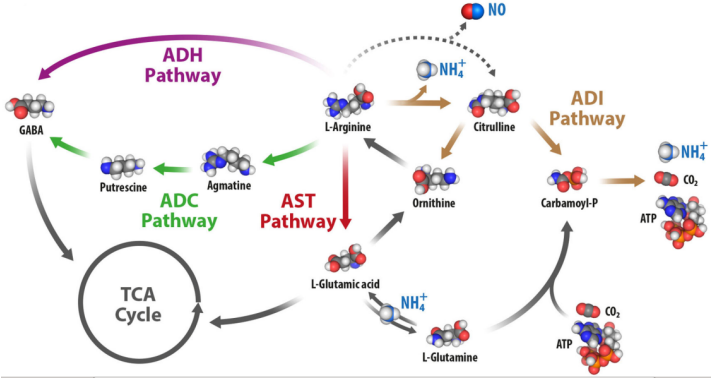

Figure 10. Schematic representation of L-arginine metabolic pathways. The pathways present in *P. aeruginosa* are indicated with continuous lines; the dashed line indicates the utilisation of arginine to produce NO by bNOS (Rinaldo et al., 2018).

These mechanisms of regulation (nutrient input, transcriptional regulation, protein-protein and protein-ligand interactions) work in combination finely controlling the c-di-GMP network and providing both specificity and fidelity to the system.

AIM OF THE WORK

In developed countries, more than 60% of human chronic infections are caused by bacterial biofilm. These communities are difficult to eradicate since they show an high resistance to both antimicrobials agents and host immune system response. One of the most important factor controlling this process is the bacterial second messenger 3',5'-cyclic diguanylate (c-di-GMP). For this reason, a deep knowledge about the c-di-GMP signalling and metabolism is crucial to develop new therapeutic approaches against bacterial biofilm.

Given that nutrients are among the major driving forces guiding the change of c-di-GMP levels, the characterization of the mechanistic details linking nutrients sensing to c-di-GMP homeostasis is very interesting and up to now poorly characterized. In particular my project has been focused on the **characterization of the Hybrid Protein RmcA from *Pseudomonas aeruginosa*.** The aim of study was to identify a putative protein in *P. aeruginosa* able to link the nutrient state to c-di-GMP signalling. To identify the best canditate we looked for a GGDEF-EAL protein harbouring the Venus Fly Trap (VFT) domain, one of the most representative fold among proteins involved in periplasmic nutrients perceiving. The Gram negative *P. aeruginosa* is the leading agent of nosocomial infections and the main cause of death in cystic fibrosis (CF) patients. The genome of *P. aeruginosa* encodes for proteins involved in c-di-GMP metabolism harbouring the GGDEF and/or the EAL signatures. Among these, *rmcA* (Redox modulator of c-di-GMP) gene encodes for a protein harbouring a periplasmic VFT sensory domain, a transmembrane helix, three Per-Arnt-Sim (PAS) domain and one light, oxygen, or voltage domain (LOV) and finally the GGDEF-EAL domains. Recent studies demonstrate that the deletion of this gene in *P. aeruginosa* PA14 strain affected the bacterial swarming and swimming motility (Okegbe et al., 2017). Few structural data are available on this family of enzymes and these data indicate that the output of this class of proteins is regulated by a reciprocal allosteric control between the two GGDEF and EAL domains occuring via inter-domain interactions and ligand-induced conformationals changes. In addition, the final output is difficult to predict since it depends also on the interaction between the two domains and the upstream sensing/regulatory ones.

In the light of this, the biochemical characterization of this protein has been divided in three different tasks:

• The identification of the environmental signal controlling the RmcA output. This goal was reached following an interdisciplinary approach including bioinformatics, biophysics and microbiology. Bioinformatic preliminary data identified the putative signal perceived by the sensory domain and this interaction was confirmed by Isothermal Titration Calorimetry (ITC). Moreover, we observed that this environmental signal triggered the protein activation *in vivo* in *P. aeruginosa* PAO1 strain.

• The unveiling of the mechanistic details of PDE catalysis control. Combining bioinformatics, enzyme kinetics, biophysics and structural biology, we characterized the biochemical properties of the GGDEF-EAL containing region of RmcA (hereinafter DUAL). DUAL has a phosphodiesterase catalytic output EAL-dependent which is regulated by the upstream GGDEF inactive domain.

• The role of LOV domain in controlling the PDE catalysis and signal transduction. Since the catalytic output of hybrid proteins is strongly regulated by the upstream domains, we characterized the biochemical properties of DUAL upstream LOV domain in order to assess its putative role in phosphodiesterase activity regulation. This goal was tested combining bioinformatics, enzyme kinetics and biophysics approaches.

During the enzymatic characterization of RmcA, we observed alternative and novel reactivity of the GGDEF domain which has been analysed more deeply, also in comparison with other GGDEF-containing enzymes. We found that DUAL protein showed an unusual catalytic activity converting GTP to GMP. We therefore investigated whether this unexpected feature is a common feature of different GGDEF containing proteins, including both DGCs and hybrid proteins. In DGCs, this side-activity occurs when the physiological diguanylate activity does not take place, due to either GGDEF dimerization issues or constitutive inactivation of DGC activity. On the other hand, in the hybrid proteins tested in this study, the unusual GTPase activity seems to compete with the main phosphodiesterase activity. This side project has been useful for the overall study presented in this PhD thesis, since it allowed us to establish the best experimental conditions to study this domain, since literature data describing GGDEF domian are really fragmentary.

The data obtained in this PhD research project allowed us to improve the knowledge concerning the regulation of GGDEF-EAL hybrid proteins, so far poorly characterized biochemically. In particular, the identification of the environmental signal perceived by the N-terminal sensory domain of RmcA represents a novel mechanism of metabolite sensing important for c-di-GMP metabolism. In addition, combining structural biology, protein engineering and enzyme kinetics, we described an allosteric mechanism regulating the phosphodiesterase output of RmcA and we showed a novel unusual kinetic activity of the GGDEF domain.

MATERIALS AND METHODS

3.1 Proteins expression and purification. *RmcA* gene was amplified by PCR from genomic PAO1 DNA and subcloned (NdeI/BamHI) as N-terminal His-tag construct in Pet28b (hereinafter RmcA FL; residues 1-1245). In addition, some constructs of RmcA were obtained by PCR of a synthetic construct of *rmcA* (GeneArt) encoding for the last 554 amino acid residues and subcloned as N-terminal His-tag constructs in Pet28b. From these templates, the fragments listed in Fig. 10 were coned. In addition, the constructs encoding for other c-di-GMP metabolizing enzymes, previously available in the laboratory, were tested (Fig. 10).

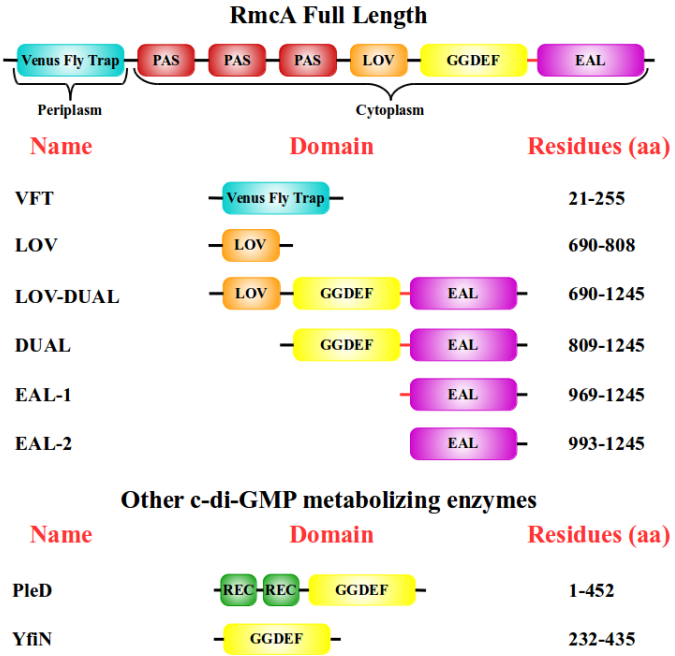

Figure 10. Domain organization of Full Length RmcA protein from *P. aeruginosa*. From the RmcA FL template, several constructs were obtained and characterized. In addition, constructs encoding for DGC enzymes and Hybrid Proteins were kinetically analyzed.

Site-directed mutants were obtained using the Quikchange Lightning kit (Agilent Technologies, Santa Clara, CA) according to the manufacturer's instructions; mutagenesis were confirmed by DNA sequencing. All constructs were overexpressed in the *E. coli* BL21 (DE3) strain. Bacterial cultures were grown at 37°C in Luria-Bertani (LB) liquid medium supplemented with 30 μg/ml Kanamycin (Sigma). When OD 600 was about to 0.8, the temperature was reduced to 20°C and protein expression was induced by adding 0.5 mM IPTG (isopropyl B-d-thiogalactoside; Sigma). Cells were harvested by centrifugation after 20 hours and stored at -20 °C. All bacterial pellets were suspended in lysis buffer and then they were lysed by sonication. After centrifugation, the proteins were purified by affinity chromatography using a HisTrap column (GE Healthcare) loaded with Ni^{2+} and equilibrated with Buffer A, specific for each protein (Table I). Elution was carried out increasing the imidazole concentration, with the proteins eluting at 150-300 mM imidazole range. Fractions containing pure protein were pooled, imidazole was removed with PD-10 desalting columns (GE Healthcare) and concentrated with Ultracel Amicon® concentrators. FL protein was only partly purified for a preliminary characterization. The other proteins were loaded on different FPLC columns, according to their molecular weights, and eluted with buffer A using an FPLC apparatus (AKTA system) (Table 1). Purified proteins were flash frozen in liquid nitrogen and stored at −20°C and the protein content was evaluated with BCA assay (Sigma-Aldrich) and spectroscopically. When affordable the Molar Extinction coefficient (ε) was calculated by BCA.

Name	Lysis Buffer	FPLC Column	Buffer A	ε ($mg \cdot ml^{-1}$)
FL	250 mM NaCl, 50 mM Tris-HCl pH 8, 1 mM PMSF,+2% v/v Tween®20 1 cOmplete protase inhibitor (Roche)	//	(20 mM Tris-HCl pH 7.5, 250 mM NaCl, +2% v/v Tween®20	2.13
VFT ; LOV	250 mM NaCl, 50 mM Tris-HCl pH 8, 1 mM PMSF and 1 cOmplete protease inhibitor (Roche)	Superdex 75	20 mM Tris-HCl pH 8.5, 150 mM NaCl	0.9 ; 1.3
LOV-DUAL	50 mM NaCl, 50 mM Tris-HCl pH 8, 1 mM PMSF and 1 cOmplete protease inhibitor (Roche)	Superdex 200	20 mM Tris-HCl pH 7.5, 300 mM NaCl	0.97
DUAL; EAL-1; EAL-2	250 mM NaCl, 50 mM Tris-HCl pH 8, 1 mM PMSF and 1 cOmplete protease inhibitor (Roche)	Superdex 200	20 mM Tris-HCl pH 7.6, 150 mM NaCl	0.6 ; 0.83 ; 0.93
PleD	20 mM Tris–HCl pH 8.0, 50 mM NaCl, 1 mM PMSF and 1 cOmplete protease inhibitor (Roche)	Superdex 200	100 mM NaCl, 20 mM Tris–HCl pH 8.0	0.3
YfiN	250 mM NaCl, 10 mM Tris-HCl pH 8, 10% v/v Glycerol, 2 mM PMSF and 1 cOmplete protease inhibitor (Roche)	Superdex 200	250 mM NaCl, 10 mM Tris-HCl pH 8, 10% v/v Glycerol	0.3

Table I. Details on composition of lysis buffer, buffer A and FPLC columns used to purify each construct.

3.2 Kinetic assay: PDE activity. PDE activity was evaluated by reverse-phase high-performance liquid chromatography (RP-HPLC), as previously described (Stelitano et al., 2013), to set the optimal buffer conditions and to probe the effect of the different nucleotides and non-hydrolyzable GTP analogues (Jena Bioscience) on PDE activity. To study the phosphodiesterase activity of the different purified constructs, a 1 μM enzyme solution was incubated at 25°C in 20 mM Tris-HCl pH 8, 100 mM NaCl, 2.5 mM $MnCl_2$ and 80 μM GTP. The reaction was started after the addition of 30 μM c-di-GMP and it was stopped at selected times by adding 150 μl of 50 mM EDTA pH 6.0 and boiled at 95°C for 10 min. Reactions were centrifuged for 10 min at 13000 rpm and the protein precipitate was removed with 0.2 μm filters (Bilk GHP Acrodisc 13mm). The reactions products were separated using a 150 x 4.6 mm reverse phase column (Prevail C8, Grace Davison Discovery Science, particle size of 5 μm) with 100 mM phosphate buffer pH 5.8/ methanol (98/2, v/v, 1 ml/min) a mobile phase and set the UV detector at 254 nm. Data are the mean of two experiments ± SD. Real-time kinetics of PDE activity were assayed by circular dichroism (CD), as previously published (Stelitano et al., 2013). Briefly, protein solution (1 μM) in 20 mM Tris-HCl pH 8.0, 100 mM NaCl and 2.5 mM $MnCl_2$ was incubated 10' at 25°C; if indicated, the mixture was further incubated 5' at 25°C with 50 μM GTP (or the concentration indicated for the GTP-dependence) prior the addiction of c-di-GMP; the reaction was carried out in 1 cm path quartz cuvette in 800 μl of final volume and followed for 10 min. C-di-GMP degradation was monitored following the CD signal at 282 nm, using a JASCO J-710 spectropolarimeter at 25°C. The values are the means of data from at least three independent experiments, and the errors are ± SD. The c-di-GMP content was extrapolated by using the calibration curve of c-di-GMP previously obtained. These data were used for the Michaelis-Menten plot; for DUAL E890A fit of kinetic data were carried out with the substrate inhibition equation, using a simple model where binding of a second molecule of substrate to the Michaelis-Menten complex yields a dead-end state:

$$V_0 = \frac{\frac{Vmax}{1 + \frac{[S]}{K_I}} \cdot [S]}{\frac{K_M}{1 + \frac{[S]}{K_I}} + [S]}$$

The hyberbolic trend of V_0 PDE (with 30 μM c-di-GMP) as a function of [GTP] was fitted with the binding equilibrium equation:

$$f\,Vmax = \frac{[GTP] + 1 + K_D - \sqrt{\left\{\left([GTP] + 1 + K_D\right)^2 - 4 \cdot [GTP]\right\}}}{2}$$

3.3 Kinetic assay: GTPase activity. The GTPase activity of different RmcA-derived constructs as well as of PleD, YfiN was analyzed using RP-HPLC. RmcA-derived constructs and YfiN (10, 8 or 5 μM, as indicated) in 20 mM Tris-HCl pH 8.0, 100 mM NaCl and 2.5 mM $MnCl_2$ were incubated with 100 μM GTP and the reaction mixture was kept at 25°C for different time intervals. The rates of hydrolase activity were also assayed in the presence of 30 or 60 μM c-di-GMP, if indicated. To test the putative GTPase activity of PleD, 5 μM of enzyme in 20 mM Tris-HCl pH 8, 100 mM NaCl and 10 mM $MgCl_2$ was incubated for 10 minutes at room temperature. The DGC activity of the enzyme was then activated by adding 10 mM NaF and 1 mM $BeCl_2$ and kept at room temperature for 30 minutes. To avoid DGC enzyme activation, the inactive form of the enzyme was obtained by not adding $BeCl_2$. Both catalytic reactions were then performed at 25°C adding 100 μM GTP. All the reactions, which were carried out with different enzymes, were stopped and the nucleotide content was separated and detected as described above.

3.4 Optimization of GMP separation by RP-HPLC. To assess the identity of the GTPase activity product, we optimized the RP-HPLC separation. We separated the unknown species using a 150 x 4.6 mm reverse phase column (Prevail C8, Grace

Davison Discovery Science, particle size of 5 µm). Due to the incompatibility of 100 mM phosphate buffer with MS analysis, catalytic products were eluted with 0.1% Formiate/Methanol (98/2, v/v, 0.3 ml/min) a mobile phase, setting the UV detector at 254 nm. The product eluted was lyophilized and Mass Spectrometry analysis was done in collaboration with Prof. Cappellacci from University of Camerino. HPLC-DAD-ESI-TRAP studies were performed using an Agilent 1100 series and an Ion Trap LC/MSD Trap SL G2445D from Agilent Technologies (Santa Clara, CA, USA) equipped with an ESI source operating in negative ionization mode.

3.5 Isothermal Titration Calorimetry (ITC) assays. Isothermal titration calorimetry (ITC) experiments were carried out using an iTC200 microcalorimeter (MicroCal). Parameters of the different titrations are reported in Table II. All titrations were carried out using both ligands and proteins in the corresponding buffer A, indicated in Table I. ITC data were analyzed by integrating the heat exchange for each addition and normalized for the amount of injected protein. The heat of binding (H), the stoichiometry (n), and the dissociation constant (K_D) were then calculated from plots of the heat evolved per mole of ligand injected versus the molar ratio of ligand to protein using the Origin software provided by the vendor (single binding site equation). Data are the mean of at least three experiments ±SD.

Protein	Ligand	Injection Volume	Injection time interval	Temperature
VFT 32 µM	Amino Acids 600 µM	1.2 µl	180 sec	25°C
DUAL 35 µM (± 25 µM GTP)	C-di-GMP 390 µM	1.2 µl	200 sec	25°C
EAL-2 25 µM	C-di-GMP 195 µM	2 µl	180 sec	25°C
LOV 10.3 µM	FAD,FMN,PYO 149.2 µM	1.5 µl	300 sec	25°C

Table II. Details on ITC parameters applied to assay the binding properties of RmcA-derived constructs.

3.6 Experiments in the presence of FAD. Flavin Adenine Dinucleotide (FAD) reconstitution experiments were performed using 10 μM of LOV-DUAL or DUAL protein in buffer A. Absorbance spectra of each construct were acquired before the reconstitution. Then, both protein were incubated with 30 μM of FAD in corrisponding buffer A for 120 minutes at 25°C. After this incubation, unbound FAD was removed using a PD Minitrap G-25 and the absorbance spectra were recorded to establish the presence of bound FAD. The titration of LOV construct with FAD was tested by fluorescence experiments performed as described by Sengupta and coworkers (Sengupta et al., 2012). Briefly, the FAD fluorescence emission quenching at 535 nm was recorder upon the addition of increased amounts of LOV protein. The time course phosphodiesterase activity in presence of FAD was tested in both anaerobic and aerobic conditions using RP-HPLC. Low oxygen tension was established by flushing with nitrogen for 30 minutes the 0.66 μM LOV-DUAL solution in 20 mM Tris-HCl pH 8, 100 mM NaCl, 2.5 mM $MnCl_2$ with 100 μM FAD and/or 100 μM GTP and the same PDE buffer containing 30 μM c-di-GMP as substrate. Both solutions were fluxed wit nitrogen keeping them into gas thight cuvettes. Subsequently, the PDE buffer containing the c-di-GMP with FAD and/or GTP was inserted into a glass micro cylinder closed with a gas thight rubber cup, previously fluxed with nitrogen, and the protein solution was added, diluting the LOV-DUAL solution to 0.33 μM final concentration. Reactions were kept at 25°C for different time intrvals, they were stopped and the nucleotide content was separated and detected as described above.

3.7 Fluorescence experiments. Titration of DUAL, EAL-1 and EAL-2 constructs with MANT-GTP and MANT-c-di-GMP (Life Technologies) was assayed on a Fluoromax-4 single photon counting spectrofluorometer (Horiba JobinYvon). Briefly, protein tryptophans were excited at 280 nm and the fluorescence emission spectra were recorded between 400 and 550 nm, as a result of Förster Resonance Energy Transfer (FRET) to MANT-GTP or MANT-c-di-GMP (in 1 cm light path; Hellma), after 3 min of incubation with the fluorophore. The binding of the fluorophores with each proteins was tested in 20 mM Tris-HCl pH 7.6, 150 mM NaCl and 2.5 mM $CaCl_2$ at 25°C in a final volume of 500 μl.

FRET experiments were performed titrating 2 μM of each proteins with MANT-GTP or MANT-c-di-GMP at different increasing concentrations and the spectra were baseline corrected by subtracting the buffer from the raw data.

3.8 MANT-GTP Displacement. The displacement of MANT-GTP was carried out following the decrease of fluorescence of the DUAL/MANT-GTP complex (1 μM and 5 μM, respectively) in 20 mM Tris-HCl pH 7.6, 150 mM NaCl and 2.5 mM $MnCl_2$ upon the addition of increased amounts of GTP, GTPαS and GTPγS. The maximum of the emission spectrum was used as fluorescence signal for displacement plot, once the value was baseline corrected. For displacement experiments, data were fitted with the following displacement equation:

$$f_x = f_{bott} + \frac{\left(f_0 - f_{bott}\right)}{1 + 10^{\left(\log x - \log K_{app}\right)}}$$

Where x is the concentration of each GTP species used for the displacement experiments, f_x is the fluorescence signal at each GTP addition, f_0 the fluorescence of the MANT-GTP/DUAL complex when no competitor is present, f_{bott} is the fluorescence of 5 μM MANT-GTP in the presence of the maximal concentration of of GTP species used for each displacement; data fit was corrected for the slope of the free MANT-GTP signal. Kapp is the displacement constant, corresponding to the concentration of competitor required to obtain 50% of displacement. K_{app} is dependent on K_{D_GTP}, $K_{D\_MANT\text{-}GTP}$ and [MANT-GTP] used in the assay according to the following equation:

$$K_{app} = K_{D\_GTP} \cdot \left(1 + \frac{\left[MANT - GTP\right]}{K_{D\_MANT - GTP}}\right)$$

RESULTS and DISCUSSION

4.1 *In vitro* characterization of the VFT domain of RmcA. The biochemical characterization of RmcA started from the study of its N-terminal sensory domain in order to identify the putative signal recognized from this hybrid protein. According to the RmcA domain organization, reported in Fig. 10, the periplasmic region (residues 23-274) could be likely involved in signal recognition and transduction. For this reason the periplasmic region of RmcA (residues 21-255) was cloned, expressed and purified as indicated in Materials and Methods. At the same time, Prof. Paiardini ('La Sapienza' University, Rome, Italy) performed a bioinformatic analysis on this domain of RmcA, which suggested that this region contains a VFT domain involved in signal recognition and transduction. The VFT domain, present in Periplasmic Binding Proteins (PBPs), can recognize a wide spectrum of nutrients including mono- and oligosaccharides, amino acids, oligopeptides and other nutrients. An homology model of the VFT domain of RmcA was built in order to describe the structure-function relationships of this domain and to identify the signal controlling RmcA activity (Paiardini et al., 2018). *In silico* analysis strongly suggested that the VFT domain of RmcA could bind L-arginine through different residues. In particular, Asp44 participates in ion-pair and ion-dipole interactions with L-arginine, while the the aromatic rings of Trp47 and Trp86 are involved in π-stacking with guanidinium group of the bound L-arginine (Fig. 11). These interactions are also crucial for the binding of L-arginine into the VFT domain of AncQR (Clifton and Jackson, 2016), supporting the scenario that RmcA could perceive the presence of L-arginine via its VFT domain.

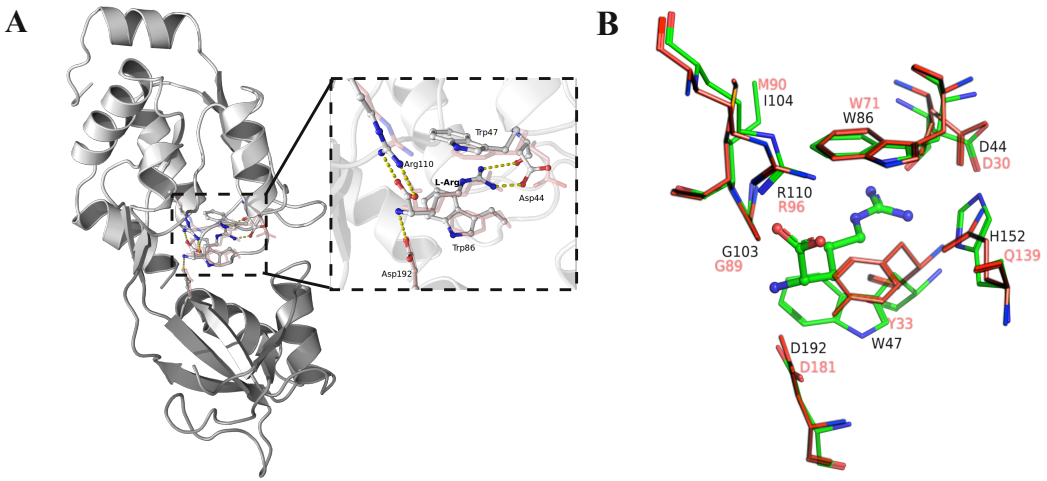

Figure 11. Homology model of the periplasmic Venus Flytrap (VFT) domain of RmcA and L-arginine binding pocket. (A) Cartoon representation of the VFT domain. Polar interactions between L-arginine and the protein moiety are shown in yellow. The corresponding positions of AncQR from *E. coli* (PDB: 4ZV1) are represented as transparent pink sticks. (B) Structural superposition between the L-arginine binding pocket in VFT model of RmcA (green sticks) and AncQR (pink sticks). Residues are labelled according to sequence numbering. Nitrogen and oxygen atoms are colored blue and red, respectively. Figures adapted from Paiardini et al., 2018.

To confirm the *in silico* homology model, a biochemical analysis was performed on this domain. The VFT domain is monomeric in solution regardless of the presence of L-arginine in the buffer (Fig. 12A). Moreover, the excess of L-arginine results in a slight but significant increase of the thermal stability of the protein (Fig. 12B) suggesting that an interaction between the VFT and this amino acid could take place.

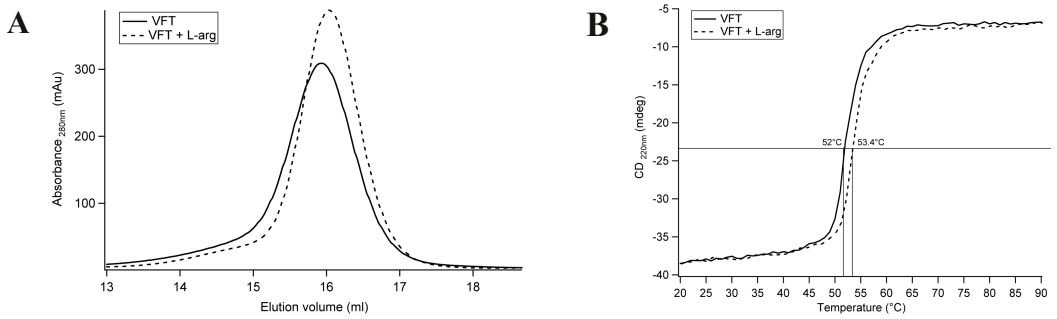

Figure 12. Structural properties of VFT. (A) Size–exclusion chromatography on a Superdex S200 10/30 column (Amersham). Chromatographic profiles of VFT samples eluted with 100 mM NaCl, 50 mM Tris pH 8.5 (continuous line) or in the presence of 1 mM L-arginine in the same buffer (dashed line), the latter after incubation of VFT with L-arginine for 10 minutes, at room temperature. L-arginine does not alter chromatographic profile of VFT, the elution volume is compatible with the monomeric protein. (B) Thermal denaturation profile of 12 μM VFT (in 150 mM NaCl, 50 mM Na/phosphate buffer pH 8.0 with or without 100 μM L-arginine, dashed and continuous lines, respectively). The Thermal melting has been followed on a circular dichroism JASCO J-710 spectropolarimeter in a 1 mm quartz cuvette (Hellma) at 220 nm. The melting curves were obtained increasing the temperature from 20°C to 90°C, with a constant rate of 1°C/min and data pitch of 1°C. Figures adapted from Paiardini et al., 2018.

The interaction between the VFT of RmcA and L-arginine was assessed by Isothermal Titration Calorimetry (ITC). VFT binds L-arginine with a K_D=11.9±0.9 μM and a stoichiometry of 0.8±0.1 per monomer (Fig. 13A) and the measured affinity is of the same order of magnitude of that of the structural template AncQR (K_{D_VFT}=11.9 vs K_{D_AncQR}=5.7 μM). The binding is highly specific for L-arginine, since no other amino acids such as lysine, leucine or glutamic acid could bind to this domain (Fig. 13A). To further validate the structural properties of L-arginine binding, the residues Asp44 and Trp47, predicted to be crucial for the interaction, were mutated into Ala and Leu, respectively. As expected, this double mutation completely abolishes the ability of VFT to bind L-arginine (Fig. 13B), confirming the predicted binding mode.

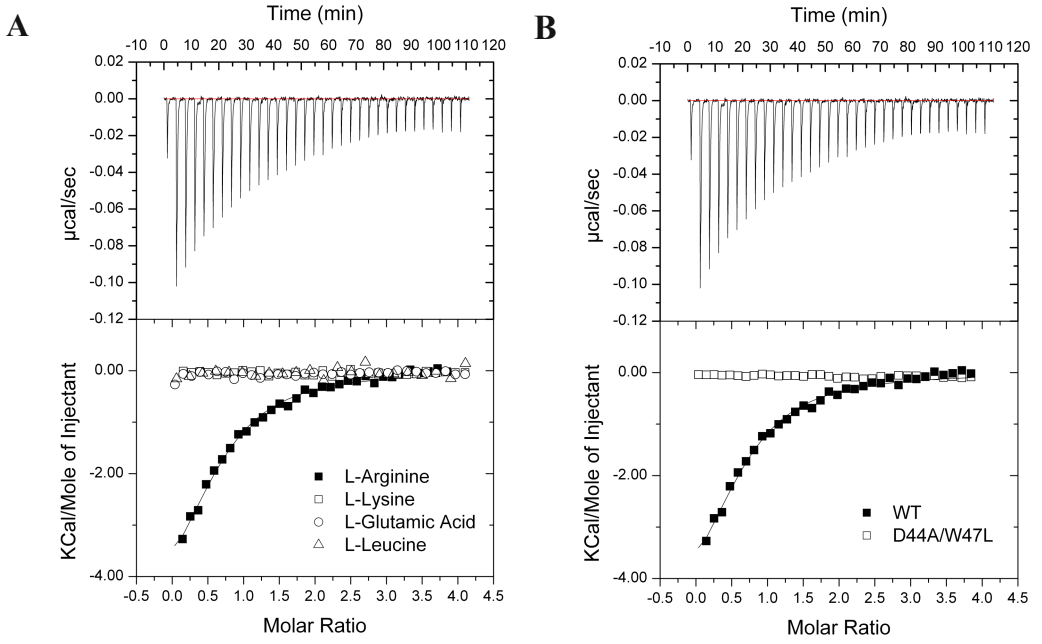

Figure 13. Binding of L-arginine to purified VFT. (A) Isothermal Titration Calorimetry (ITC) was carried out by titrating a VFT with different amounts of L-arginine at 25 °C in corrispondent Buffer A. To verify the specificity of binding, wild-type VFT was titrated with other amino acids, as indicated in the figure legend, under the same experimental conditions. Data were fitted with the single binding site equation with the Origin software, as provided by the vendor (continuous line), yielding the following parameters: n=0.8±0.1; K_D=11.9±0.9 µM; ΔH=-4.3±0.3 kcal/mol; ΔS=8.0±0.9 cal/mol/deg. (B) Titration was repeated with the D44A/W47L double mutant of VFT, under the same experimental conditions. Figure adapted from Paiardini et al., 2018.

4.2 RmcA responds to L-arginine modulating c-di-GMP levels. To test the possible effect of L-arginine in modulating RmcA activity *in vivo*, the intracellular levels of c-di-GMP were indirectly evaluated using an *ad hoc* biosensor (Pawar et al., 2016). Our collaborator Dr. Rampioni (Roma Tre University, Rome, Italy) and his group used the wild type *P. aeruginosa* PAO1 and Δ*rmcA* mutant strain deleted in the *rmcA* gene for phenotypic characterization. C-di-GMP levels are 50% higher in the Δ*rmcA* strain relative to wild type when L-arginine is used as carbon source and this phenotype is complemented by the constitutive expression of RmcA *via* the pUCP18-derived plasmid p*rmcA* (Fig. 14A). As expected, when using M9 medium supplemented with lysine, glutamic acid, or leucine as sole carbon sources, no significant difference is observed between the wild-type and Δ*rmcA* mutant (Fig. 14A). These data indicated that likely RmcA is involved in lowering c-di-GMP levels, and therefore it is likely a PDE responsive to arginine. In line with our observations, the recent characterization of RmcA counterpart in PA14 strain showed that indeed this protein is a PDE even though the environmental cue controlling its activity was not identified (Okegbe et al., 2017). Since a reduction in intracellular c-di-GMP levels negatively affects biofilm formation (Römling et al., 2013), we analyzed the effect triggered by L-arginine and the other amino acids on the biofilm formation in PAO1 wild type and Δ*rmcA* strains. Using L-arginine as sole carbon source, biofilm adhesion units were ~12% higher in PAO1 Δ*rmcA* respect to PAO1 wild type, while ~35% lower in PAO1 Δ*rmcA* carrying the p*rmcA* plasmid compared to the same mutant strain carrying the empty vector pUCP18 (Fig. 14B). As previously showed for the c-di-GMP levels, no phenotypic differences are observed when lysine, glutamic acid, or leucine are used as carbon sources (Fig. 14B). Our *in silico* data proposes that RmcA binds to L-arginine *via* its VFT domain and this binding triggers the protein activation resulting in a reduction of c-di-GMP levels and of biofilm formation *in vivo*, strongly suggesting that RmcA acts as a PDE. In accordance with these data, we found that *in vitro* the partially purified full-length RmcA protein shows the PDE activity, but not a significant DGC one (Fig. 14C). These findings support the idea that RmcA is a sensory one-component system coupling the L-arginine sensing and the intracellular levels of the second messenger c-di-GMP.

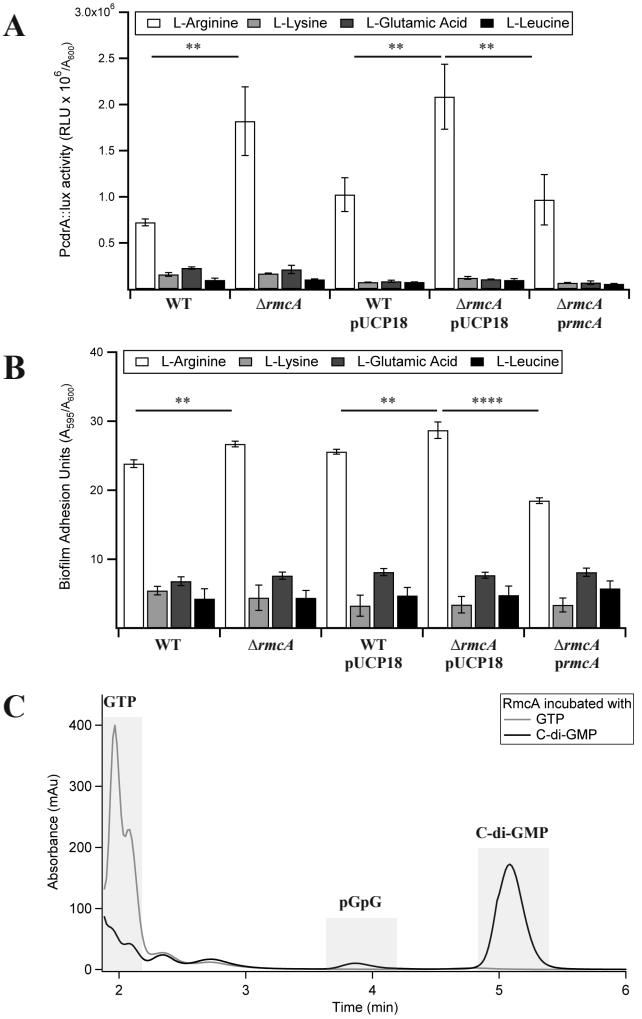

Figure 14. RmcA acts as a PDE *in vivo* and *in vitro*. (A) The c-di-GMP levels were evaluated using *PcdrA::lux* reporter system in the indicated strains using M9 minimal medium supplemented with 20 mM of different amino acids, as indicated in the figure legend, as sole carbon sources. *PcdrA::lux* activity was calculated as RLU normalized to A_{600}. (B) For biofilm formation assays, wild type and ΔRmcA strains containing or not the pUCP18 empty vector or pRmcA plasmid were grown in M9 minimal medium supplemented with 20 mM L-arginine, L-lysine, L-glutamic acid or L-leucine as

sole carbon sources. Biofilm adhesion units were calculated as A_{595} normalized to A_{600}. (C) Pilot enzymatic assays on partially purified full length RmcA. The nucleotide content of the reaction mixture, containing RmcA in the presence of excess GTP (dashed line), or c-di-GMP (continuous line), was separated by RP-HPLC to assess either the DGC or the PDE activity, respectively. While the PDE reaction yields the expected product (i.e. pGpG), no c-di-GMP accumulates starting from GTP, under these experimental conditions. Figures adapted from Paiardini et al., 2018.

4.3 GTP is an allosteric regulator of the RmcA PDE activity. To confirm the phosphodiesterase catalytic output of RmcA protein suggested by *in vivo* experiments, we produced different constructs bearing both putative catalytic GGDEF and EAL domains (DUAL) or only the EAL domain with or without the upstream hinge helix (EAL-1 and EAL-2, respectively) (Fig. 10). Given that the signature sequences of both GGDEF and EAL domains were conserved, in principle the DUAL construct is competent to carry out both the DGC and the PDE catalytic activities. We found that the DUAL protein is able to convert c-di-GMP into pGpG *in vitro* and this PDE activity is a feature of the EAL domain, in both the EAL-1 and EAL-2 constructs (Fig. 15A). In addition, under the same experimental conditions, the DUAL construct did not show neither a DGC activity nor a PDE-b activity, i.e. hydrolytic conversion of pGpG into GMP (Stelitano, 2013), using GTP as the sole substrate (Fig. 15B). Interestingly, the presence of excess GTP upregulates the PDE activity of DUAL (Fig. 15C and 15D ; Table III); this kinetic enhancement occurred also when GTP is added during c-di-GMP hydrolysis, confirming that a c-di-GMP feedback inhibition does not take place (Fig. 15E). Moreover, this positive effect induced by GTP is specific since GDP, ppGpp and pppGpp are unable to trigger EAL activation to the same extent (Fig. 15F).

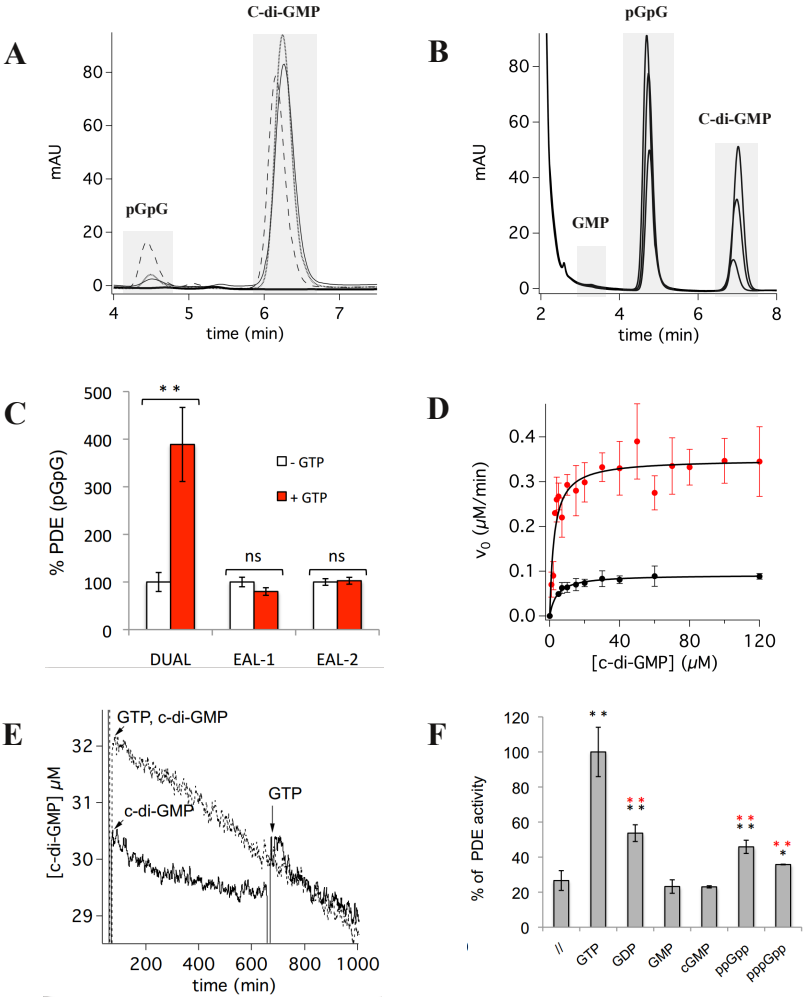

Figure 15. RmcA GGDEF-EAL construct is a GTP-dependent PDE. (A) Pilot enzymatic assays of the RmcA catalytic constructs. The nucleotide content of the reaction mixture, containing DUAL incubated with excess of GTP (bold line), or with excess of c-di-GMP (thin line), to assess the either the DGC or the PDE activity, respectively, was separated by RP-HPLC. While the PDE reaction yields the expected product (i.e. pGpG), no c-di-GMP production was detected starting from GTP, under these experimental conditions. The PDE activity was also detected on EAL-2 (dashed line) and EAL-1 (dotted line) incubated with excess c-di-GMP. (B) Nucleotide content of the reaction of

DUAL with c-di-GMP at different time (30', 60', 120'). Arrows indicate the consuption of c-di-GMP and the production of pGpG while no GMP accumulates. (C) PDE activity of each construct carried out in the presence of c-di-GMP as substrate with or without GTP (white and red bars, respectively). Values are normalized to the activity without GTP. (D) Determination of the kinetic parameters of DUAL. The PDE activity of DUAL was characterized both in the presence and in the absence of GTP (initial rate, V_0, red and black circles, respectively) as function of c-di-GMP concentration; data were fitted with the Michaelis-Menten equation (continuous line). (E) PDE time-course of DUAL and c-di-GMP: after 10 min from the beginning of the kinetics, GTP was added and kinetics followed for further 5 min (continuous trace). The increased rate of c-di-GMP consumption due to GTP addition is comparable to that observed when DUAL is incubated with excess GTP from the beginning of the kinetics (dotted trace). (F) PDE activity was carried out in the presence of different nucleotides, indicated in the X-axis. Values are normalized to the activity with GTP. Figures adapted from Mantoni et al., 2018

The GTP allosteric regulation of the PDE activity of DUAL requires the GGDEF domain. We used MANT-GTP (Biolog) as a fluorescent GTP analogue to find, by FRET spectroscopy, that GGDEF binds GTP with a 1:1 stoichiometry (one molecule/monomer). The nucleotide targets specifically the GGDEF since no binding occurs performing the titration with EAL construct (Fig. 16A); we also observed that the presence of excess c-di-GMP has no effect on MANT-GTP binding (Fig. 16B). The MANT-GTP titration by FRET spectroscopy was carried out using different amonuts of DUAL protein (Fig. 16C). We observed that the amount of MANT-GTP required to saturate the protein, reaching the fluorescent plateau, depends of DUAL concentration: this profile is typical of a titration plot indicating that DUAL protein shows a sub-micromolar affinity to MANT-GTP (Fig. 16C).

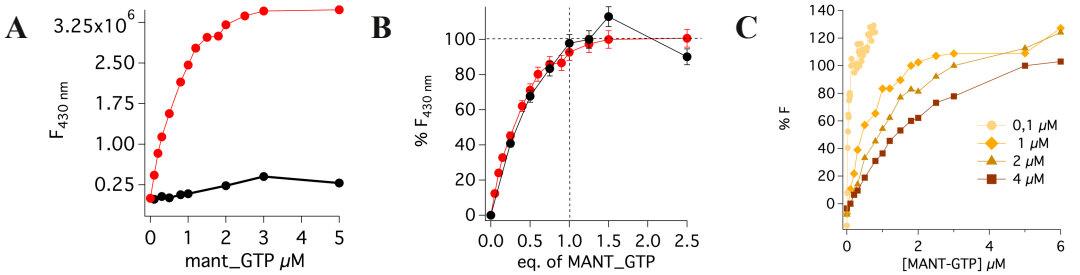

Figure 16. Binding of GTP to DUAL domain. (A) Comparison of the binding curve of MANT-GTP to DUAL (red circles) and EAL-2 (black circles). No binding was observed with the latter construct. (B) Titration of DUAL with MANT-GTP (red circles) yields a stoichiometry ratio of 1 GTP:1 DUAL monomer; the same profile was observed in the presence of excess c-di-GMP (black circles). On the Y-axis is reported the FRET signal at 430 nm normalized for the plateu value (100% of bound species) at given ligand concentration. The plateau value is considered as the Y-intercept of the line parallel to X-axis fitting the plateau points. (C) Flurescence profiles of MANT-GTP titration performed with different amounts of DUAL protein, as indicated in the legend. Figures adapted from Mantoni et al., 2018

FRET displacement experiments showed that GTP displaces MANT-GTP, confirming the sub-μM affinity also for the physiological GTP ligand (Fig. 17A). Moreover, kinetic experiments indicated that the PDE activity shows an hyperbolic dependence on GTP concentration in the tested range (2-50 μM, Fig. 17B), with an apparent K_{D_app}=2.8±0.5 μM. In contrast to the observed sub-μM binding affinity, the maximal GTP-mediated PDE activation is obtained when GTP concentration is above ~15 μM (Fig. 17B); this result implies that the GTP-dependent phosphodiesterase activation (measured by the K_{D_app}) requires additional events after the GTP binding, likely a conformational change between an inactive to an active form (OFF → ON). In agreement with this scenario, GTP enhances the V_{max} of the PDE reaction while K_M for c-di-GMP is not affected (Table III), indicating that the GTP increases the population of the catalytically competent PDE enzyme (i.e. the ON form).

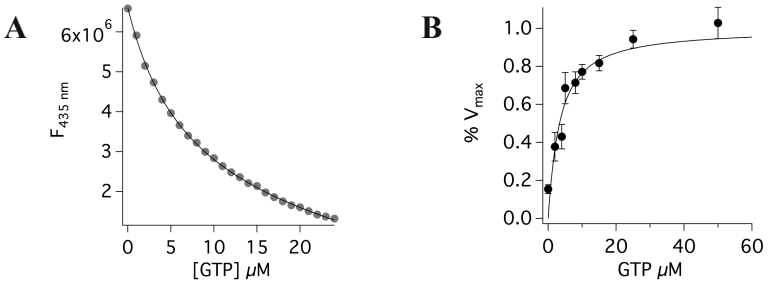

Figure 17. GTP binding effects on DUAL PDE kinetics. (A) Binding of GTP to DUAL was assayed by displacement of MANT-GTP. The competition experiment was carried out in the presence of a constant concentration of MANT-GTP and increasing competitor concentrations; buffer conditions are those optimized for PDE activity. Data were fitted (continuous lines) with the displacement equation, reported in Materials and Methods section, yielding the following K_{displ}: 6.9±0.1 μM for GTP. At this stage we cannot extrapolate the precise K_d for each competitor, since we do not know the exact $K_{d\_MANT\text{-}GTP}$. (B) The PDE activity was assayed at different GTP concentrations; the ratio $V_{0\ obs}/V_{max}$ as a function of GTP concentration is reported (black circles). Data were fitted with the reversible binding equation (continuous line). Figures adapted from Mantoni et al., 2018

RmcA Construct	GTP (μM)	$K_{M\_C\text{-}di\text{-}GMP}$ (μM)	k_{cat} (min^{-1})
DUAL	// 4 8 50	4.1±0.4 2.5±0.9 4.2±1.2 2.5±0.5	0.09±0.02 0.2±0.1 0.3±0.2 0.35±0.01
EAL-2	//	5.9±0.8	0.66±0.2
DUAL E890A	// 50	11.6±3.5 9.6±0.1	0.1 * 0.54 *

Table III. Comparison of the kinetic parameters different RmcA constructs. The GTP-dependent kinetic regulation is mediated by both lowering the K_M for the substrate as well as by increasing the turnover rate of the enzyme. * To fit these data, the V_{max} parameter has been imposed; this value falls within the range of the V_{max} observed for the wild-type construct. This constraint represents the hypothetical V_{max} of catalysis, if the substrate inhibition does not take place. For this reason, it is not a real K_{cat} but an extrapolated V_{max}, yielding the K_M values reported in the table. Data fit has been done considering one monomer of the EAL as the active site, to simplify the model.

Using ITC and FRET spectroscopy, we described the c-di-GMP binding to the EAL domain (EAL-2). As acknowledged by the literature, the first points of the titration have not been considered in the fit, being biased by the endothermic contribution due to c-di-GMP dilution into the cell (Matsuyama et al., 2016), c-di-GMP binding to EAL domain shows one binding site per monomer yielding a $K_{D\ c\text{-}di\text{-}GMP}$=171±30 nM (Fig. 18, panels A-B, including ITC and FRET data, respectively). Interestingly, the ITC titration of DUAL/c-di-GMP interaction shows a V-shaped titration profile which is indicative of sequential binding events, including the dilution of c-di-GMP and, probably, a conformational transition occurring upon binding. Due to the complex ITC profile of DUAL/c-di-GMP interaction, we described this binding by FRET spectroscopy using MANT-c-di-GMP (Biolog), a fluorescent analogue of c-di-GMP. The FRET titration shows a sub-μM affinity for MANT-c-di-GMP and 0.6:1 stoichiometry (Fig. 18B). To confirm that MANT-c-di-GMP binds specifically to the EAL active site, MANT-c-di-GMP titration was carried out also with the DUAL double mutant D1136N-D1137N, in which the mutations alter the key residues involved in metal-dependent binding of c-di-GMP to EAL active site. As expected, the double mutation (D1037N/D1038N) abolishes the c-di-GMP binding, confirming that this nucleotide targets only EAL domain (Fig. 18B). To describe the allosteric regulation mediated by GTP, we tested the c-di-GMP binding to EAL domain in the presence of GTP. Interestingly, the pre-incubation of DUAL with excess of GTP changes the stoichiometry of binding of MANT-c-di-GMP from 0.6:1 to 1:1, as in EAL/c-di-GMP FRET titration, while the ITC profile does not change significantly (Fig. 18B and 18C). Both kinetic and binding data indicated that the DUAL PDE activity is enhanced upon the presence of GTP which is able to change c-di-GMP binding stoichiometry, likely through a conformational rearrangement.

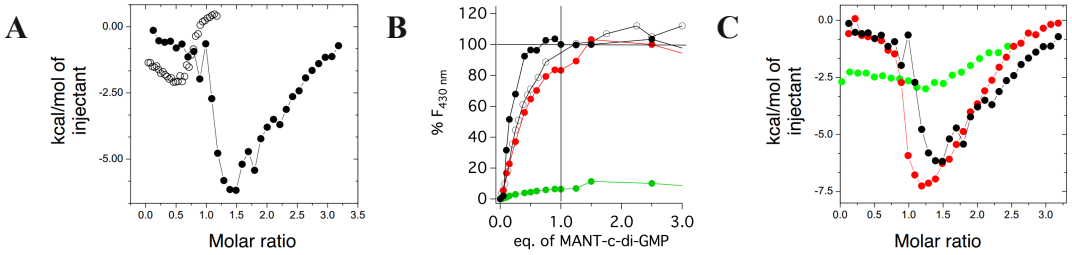

Figure 18. Binding of C-di-GMP to DUAL domain. (A) Binding of c-di-GMP to EAL-2 (open circles) and to DUAL (black squares) was assayed by ITC; the heat exchange/mol of injectant has been reported in the figure and data were fitted with a single binding site equation. (B) Binding of MANT-c-di-GMP to DUAL and EAL-2 (black and empty circles, respectively) assayed by FRET titration. The titration of DUAL was performed also after pre-incubation with GTP (red circles); the MANT-c-di-GMP titration was carried out also with the DUAL double mutant D1136N-D1137N (hereinafter DUAL_DD) and no significant binding is observed, (green circles). On the Y-axes, the % of FRET signal at 430 nm is reported considering the plateau value as 100 %. (C) Binding of c-di-GMP to DUAL as assayed titrating DUAL with c-di-GMP, with or without incubation with GTP (red and black circles, respectively). ITC was also carried out with the mutant DUAL_DD (green circles). Figures adapted from Mantoni et al., 2018.

4.4 Effect of the GTP binding on DUAL structure. Dr. Giardina and Dr. Brunotti ('La Sapienza' University of Rome) solved the structure of the DUAL construct in complex with two molecules of GTP and five calcium ions at 2.8 Å resolution. DUAL crystallized as an asymmetric dimer: the orientation of the GGDEF domain with respect to the EAL domain is very different between the two monomers (Fig. 19A and 19B). In monomer-A, the GGDEF and EAL domains are spatially closer (closed conformation) as compared to the other chain where the two domains are more distant (monomer-B, open conformation). The fold of the GGDEF and EAL domains is conserved in both monomers and the structural superposition of the two EAL domains suggests that the conformational change is achieved *via* a rigid body movement involving the connecting helix.

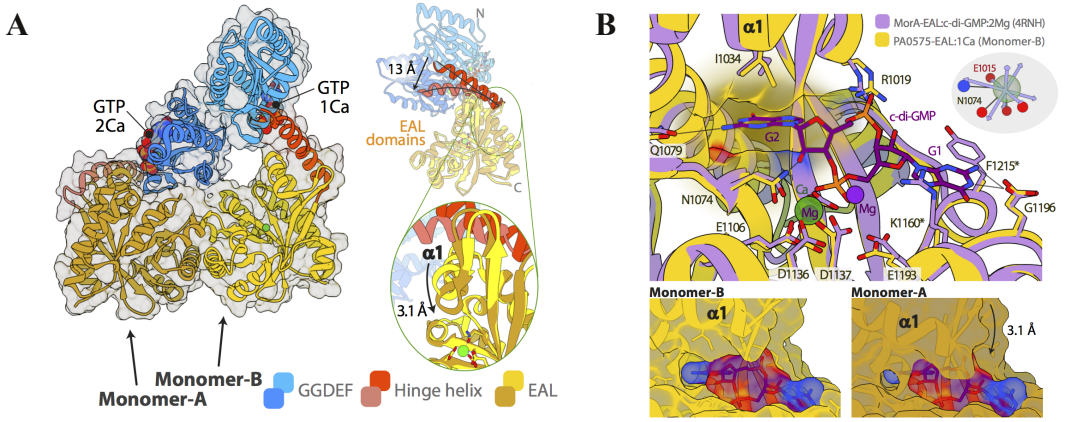

Figure 19. Structure of DUAL. (A) Structure of the DUAL asymmetric dimer (PDB: 5M3C). In each monomer the N-terminal GGDEF (blue), the connecting helix (red) and the EAL domain (yellow) are highlighted in different colours while the GTP molecules and calcium ions are shown as spheres. Superposition of the two monomers showing the conformational differences in the relative orientation of the GGDEF domain with respect to the EAL domain. The bending of the connecting helix and the corresponding shift of helix α1, belonging to the EAL domain, is highlighted in the blow-up. (B) The c-di-GMP binding site. Superposition of the EAL domain of RmcA-DUAL (open monomer, yellow) with the homologue hybrid protein from *P. aeruginosa* MorA in complex with c-di-GMP and two Mg^{2+} ions (Phippen et al., 2014 ; 4RNH, violet). One guanine docks in a hydrophobic cleft flanked by helix α1 and in the closed conformation the shift of this helix seals the cleft, making c-di-GMP binding impossible. Figures adapted from Mantoni et al., 2018.

This asymmetric structure of DUAL, where only one subunit is competent for substrate binding (monomer-B), explains the observed stoichiometry of MANT-c-di-GMP binding to DUAL (~0.6 molar ratio). Since DUAL is fully saturated by MANT-c-di-GMP in the presence of GTP, binding of the latter to GGDEF domain induces a conformational change likely opening the active site in the EAL domain (monomer-B like conformation). In agreement with this interpretation, an increase of the DUAL volume in solution upon GTP binding is also observed by Dynamic Light Scattering and Analytical Size Exclusion Chromatography (Fig. 20A and 20B, respectively).

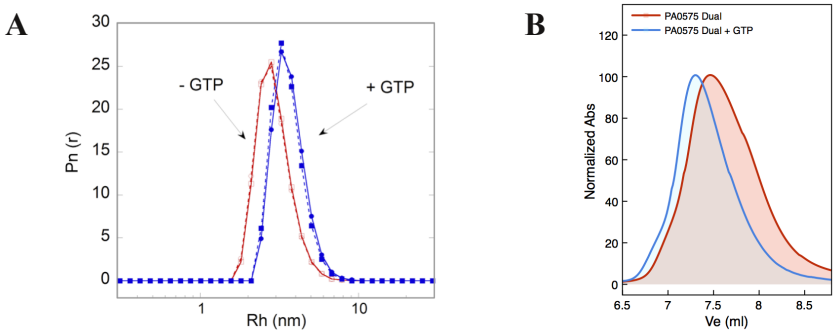

Figure 20. Structural effects of GTP on DUAL. (A) Dynamic light-scattering measurements. Hydrodynamic radius (Rh) and number distribution (Pn) of the 4 μM protein in the PDE buffer, both in the absence and in the presence of GTP at a final concentration of 50 μM. Both conditions have been tested twice, and each measurement is the result of the average of 24 consecutive measurements. Measurements were carried out with a Zetasizer Nano S (Malvern Instruments, Malvern, UK) equipped with a 4 mW He–Ne laser (633 nm), at 25°C, at an angle of 173°C from the incident beam. Peak-intensity analyses were used to determine hydrodynamic radius number distribution (Pn). (B) Size-exclusion chromatography on Superdex S200 10/30 (Amersham) on FPLC apparatus. Chromatographic profiles of DUAL samples eluted with 20 mM Tris pH 7.6, 150 mM NaCl, 2.5 mM $MnCl_2$, 2.5 mM $MgCl_2$ (red line) or in the presence of 300 μM GTP in the same buffer (blue line), the latter after incubation of DUAL with GTP for 10 minutes. GTP triggers a population of DUAL (GTP-bound) with a significantly higher hydrodynamic volume than the GTP-free form. Figures adapted from Mantoni et al., 2018.

All the results presented so far show that GTP binding to the GGDEF domain triggers a significant effect on the overall conformation of DUAL, clarifying the basis of GTP-dependent regulation of phosphodiesterase activity. Since GTP binds to both open and closed monomer, the asymmetric dimer of DUAL may indeed represent two intermediate snapshots of the events following GTP binding and leading to the fully active ON species.

4.5 Analysis of GTP binding properties in the GGDEF active sites. To develop a model of the GTP-dependent allosteric activation of RmcA, the open and closed conformations of DUAL (Fig. 19A) was analysed to model the dimeric ON and OFF states, respectively. In the closed conformation (monomer-A), the α1-helix of

the EAL domain is close to the GTP binding site of the GGDEF domain (Fig. 21). In this position, the negatively charged residues of the α1-helix may interact with the metals in the active site of the GGDEF domain, stabilizing the OFF conformation. Structural and *in silico* analysis indicated that the binding of GTP may, therefore, trigger the PDE catalysis of DUAL *via* the displacement of EAL domain releasing the GGDEF-EAL interaction and allowing the monomer to achieve the ON conformation. This large conformational rearrangement likely needs the reorganization of the GTP molecule in the GGDEF binding site, mainly at the level of the α-phosphate.

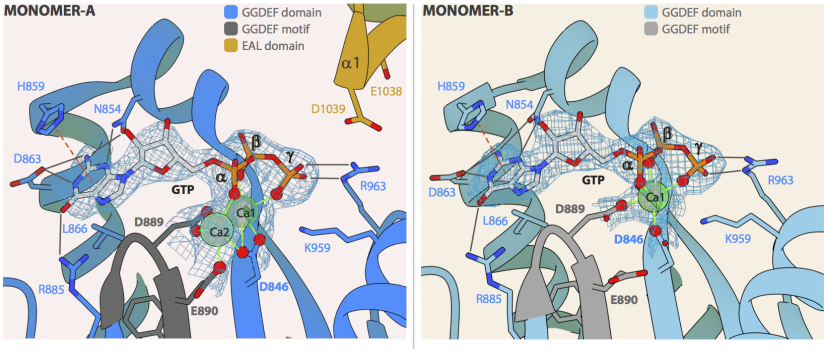

Figure 21. GTP likely triggers EAL-displacement. GTP bound to the GGDEF domain in the open monomer (right) and to the closed monomer (left).The closed monomer contains two calcium ions (Ca1 and Ca2), while in the open subunit only one ion is observed, in the same position corresponding to Ca1. Figure adapted from Mantoni et al., 2018.

To confirm this hypothesis, we tested whether the GTP-α-S, whose binding geometry is different from the GTP one, promotes the PDE activation likewise the GTP. As expected, the α-substitution does not reproduce the positive effect of GTP on PDE activity. In addition the α-substitution reduces DUAL affinity for GTP (K_{displ}:14.6±0.6 μM for GTP-α-S in contrast to K_{displ}:6.9±0.1 μM for GTP). On the other hand, the GTP-γ-S promotes PDE activation to the same extent of GTP and this γ-substitution enhances DUAL affinity for GTP (K_{displ}: 3.3±0.1 μM for GTP-γ-S in contrast to K_{displ}:6.9±0.1 μM for GTP) (Fig. 22A and 22B). The GTP-α-S analogue affects MANT-c-di-GMP binding, whose titration resembles

that observed without GTP (Fig. 22C). Thus, these data indicates that the α-substitution likely alter the geometry of binding thus hampering the formation of a PDE-catalitically competent conformation; this observation confirm our structural hypothesis showing that the GTP α-moiety is crucial to trigger EAL unlocking and dimerization.

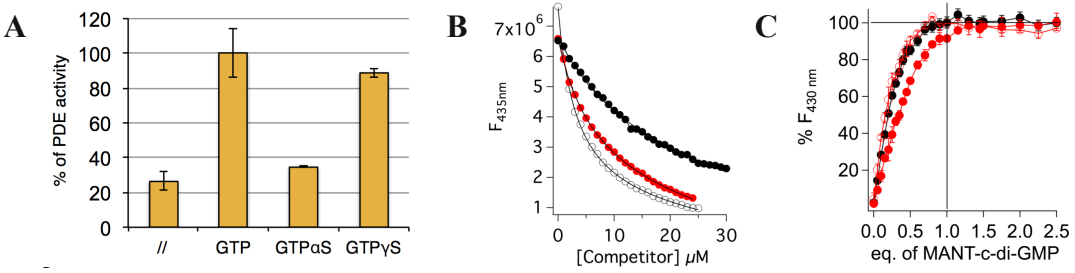

Figure 22. The α-phosphate moiety is crucial to trigger GTP-dependent PDE activation. (A) PDE activity of DUAL at 30 min after substrate addition carried out with c-di-GMP and, when indicated, with either GTP or GTP-α-S or GTP-γ-S; pGpG content was determined by RP-HPLC. Values are normalized considering the activity with GTP the maximal one (100%). (B) Binding of GTP and its analogues to DUAL assayed by displacement of MANT-GTP. The competition experiment was carried out in the presence of a constant concentration of MANT-GTP and various competitor concentrations (i.e. GTP, red circles; GTP-γ-S, white circles; GTP-α-S, black circles); buffer conditions are those optimized for PDE activity. (C) Titration of DUAL with different amounts of MANT-c-di-GMP in the presence of GTP-α-S (open circles) is compared with the experiments carried out with or without GTP (black and red circles, respectively). On the Y-axes, the % of FRET signal at 430 nm is reported considering the plateau value as 100 %. Data are the mean of three independent experiments ± standard deviation. Figures adapted from Mantoni et al., 2018.

In order to understand the contribution of the environment around the GTP α-bond moiety, we mutated the glutamic acid residue of the GGDEF signature (Glu890), involved in the coordination of the second metal ion which bridges the α-PhO group in the monomer-A (Fig. 21). The PDE activity of the DUAL E890A was characterized kinetically in presence and absence of GTP. Interestingly, the dependence of V_0 on substrate concentration yields a bell-shaped curve, indicative of substrate inhibition (Fig. 23A), with a K_i for c-di-GMP close to the apparent K_M (17.8 vs 9.6 μM, with GTP) (Table III). The mutant is still able to respond to GTP, but above 10 μM c-di-GMP, E890A is not able to maintain the PDE activation

triggered by GTP and the turnover drops significantly ~100 sec after substrate addition (Fig. 23B). Moreover, the binding of GTP to DUAL E890A does not alter the c-di-GMP binding to EAL domain, while this effect is clearly shown by the wild-type DUAL protein (Fig. 23C). This last property is not due to changes in GTP affinity, which is not significantly altered in the mutant E890A (Fig. 23D).

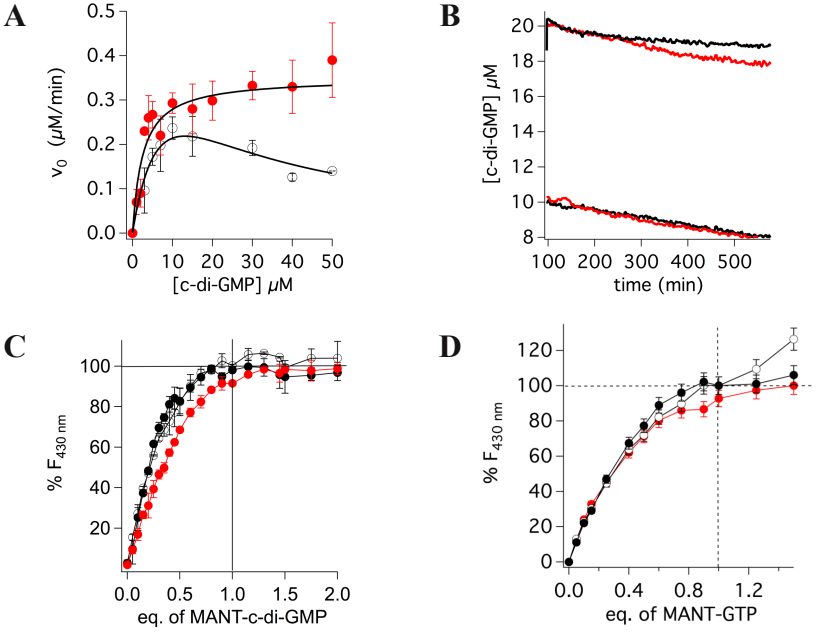

Figure 23. The GGDEF E890A mutation affects the phosphodiesterase activity. (A) The initial rate of PDE kinetics of E890A carried out in the presence of GTP was plotted as a function of c-di-GMP concentration and compared to that of DUAL (empty and red circles, respectively). Mutant kinetic data were fitted with substrate inhibition equation. (B) Time-course of PDE kinetics obtained at different c-di-GMP concentrations with DUAL WT or E890A (red and black traces, respectively). (C) Titration profile of the binding of E890A with MANT-c-di-GMP, both in the presence or in the absence of excess GTP (black or open circles, respectively); the GTP does not increase the equivalents of MANT-c-di-GMP bound, as observed in the wild-type protein (red circles). (D) Titration profile of the interaction of E890A to MANT-GTP (open circles). The profile superposes with that of the wild-type protein (red circles); the same profile was observed in the presence of c-di-GMP (black circles). The Y-axis is the % of FRET signal at 430 nm considering the plateau value as 100 %. Figures adapted from Mantoni et al., 2018.

The kinetic properties of E890A mutant resembles previously characterized kinetic behaviours of mutations localized in the dimerization helix of other EAL PDEs; in these cases, the substrate inhibition profile was due to the presence of c-di-GMP bound to one monomer, which negatively affected the catalytic efficiency of the other EAL monomer (Rao et al., 2009). We propose that the effect of the E890 mutation is propagated to the EAL/EAL interface, altering the PDE kinetic behaviour. This is the first evidence of a mutation in the GGDEF signature affecting the EAL/EAL crosstalk, resulting in uncoupling of GTP binding and PDE activation. Moreover, the kinetic profile of this E890A mutant suggests that the EAL/EAL dimerization is one of the step occurring during the GTP-dependent protein activation and this strongly supports our activation model.

4.6 Structure-based allosteric model of GTP-dependent activation of RmcA. Structural data indicate that DUAL shows two different conformational states associated by a low and high PDE activities. Specifically, the DUAL monomers are characterized by a different bending of the hinge helix connecting the GGDEF and EAL domains (Fig. 19A) suggesting that the ON→OFF transition likely involves the rearrangement from an elongated to a compact conformation. To mechanistically describe the conformational transition resulting in the allosteric activation of DUAL, Prof. Paiardini (‘La Sapienza’ University of Rome) modelled two hypothetical fully ON and OFF conformations of RmcA (Fig. 24), using our structural data and the structure of the homologous protein MorA (~65% sequence identity; Phippen et al., 2014), solved as a symmetric dimer.

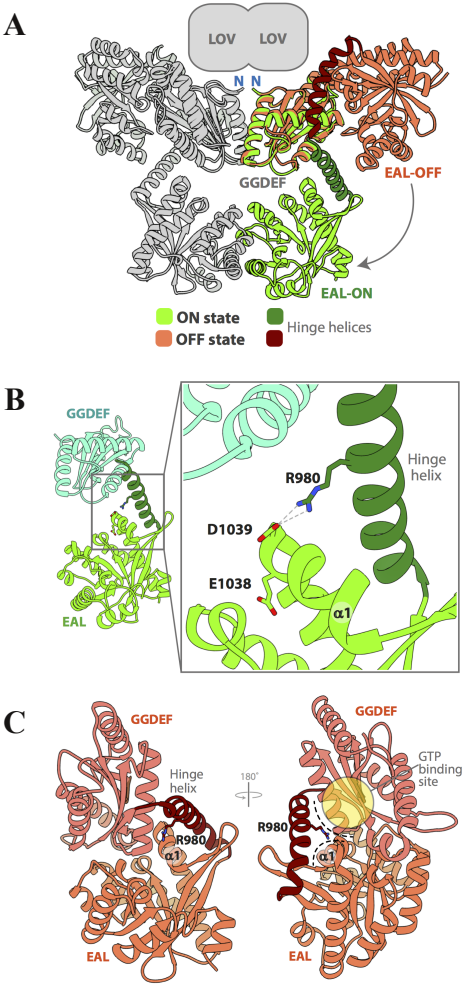

Figure 24. GTP-induced PDE activation. (A) Comparison of the symmetric dimers of the DUAL ON model (derived form the structure of MorA, green) and the DUAL OFF model obtained by NM analysis starting from the structure of monomer-A (pink). (B) Model of one monomer in the open (ON) conformation. The hinge helix is in an elongated conformation separating the GGDEF from the EAL domain. In this ON conformation Arg980 is in close contact with both Asp1038 and Glu1039. (C) Model of one monomer in the closed (OFF) state. The GGDEF and the EAL domains are in close proximity and Arg980 makes contacts with both the GTP binding site (highlighted) and the EAL domain at the level of α1. Figures adapted from Mantoni et al., 2018.

According to the OFF and ON models, the α1-helix of the EAL domain in monomer-A is closer to the GTP binding site with respect to monomer-B, suggesting that GTP binding likely triggers the reorganization of the neighboring residues in the GTP binding site, inducing the conformational OFF→ON switch. In addition, the residue Arg980, located at the centre of the hinge helix, is involved in contacts with both the GGDEF and EAL domains, linking their interactions only in the OFF state (Fig. 24C). In our model, the GTP binding induces a rearrangement of the Arg980-mediated GGDEF-EAL domains contacts likely destabilizing the OFF state and leading the opening of the DUAL module. In addition, Arg980 can also stabilize the ON state, via its interactions with residues Glu1038 and Asp1039 of the EAL domains (Fig. 24B). In agreement with this model, GTP "unlocks" the EAL domains allowing their dimerization and activation, via a large conformational change of the hinge helix (Fig. 24A). We mutated the Arg980 residue likely involved in stabilizing both the OFF and the GTP-derived ON conformations, in order to assess this mechanistic model. Interestingly, the DUAL R980S mutant shows a GTP-independent PDE activity which is higher than the catalytic activity of the GTP-free wild-type DUAL (Fig. 25). This data indicates that the substitution of this residue uncouples GTP binding from enzyme activation. In the absence of GTP, the OFF→ON equilibrium of the wild-type mainly populates the OFF state thus accounting for the low basal activity observed; on the other hand, the R980S mutation shifts this equilibrium to favour the ON state likely by destabilizing the OFF conformation. Despite this, the R980S mutant PDE activity is slightly lower than that of the wild-type protein in the presence of GTP (Fig. 25).

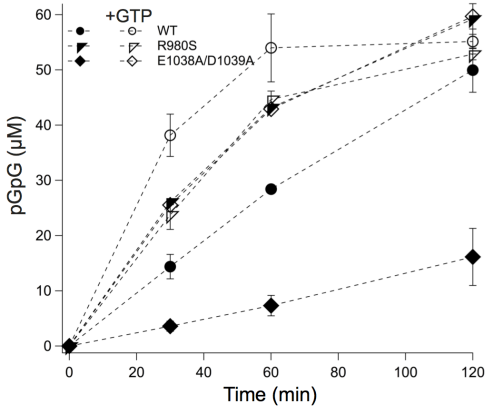

Figure 25. Kinetic analysis of GTP activation as suggested by OFF-ON transition model. PDE activity of 10 μM wild-type (circles), R980S (triangles) and E1038A/D1039A (diamonds) DUAL carried out in the presence of 60 μM c-di-GMP as substrate with or without 100 μM GTP (empty and black symbols, respectively). Nucleotide content of each mixture was assayed by RP-HPLC after 30 min of reaction at 25°C. Data are the mean of at least two experiments ±SD. Figure adapted from Mantoni et al., 2018

This kinetic behaviour could be explained, according to the model, by the fact that Arg980 is also involved in electrostatic interactions with Glu1038 and Asp1039 in the ON state, stabilizing the ON conformation. Nevertheless, the GTP insensitive behaviour of R980S mutant indicates that the Arg980 residue is involved to 'lock' DUAL in the OFF state. To further validate our structural hypothesis, we modified conserved residues involved in stabilizing the ON state, i.e Glu1038 and Asp1039, which could interact with Arg980 in the ON structure. As expected, in the presence of excess GTP, this E1038A/D1039A double mutant shows a PDE activity similar to the R980S mutant, being also in this case clearly lower than that observed in the GTP-containing wild-type protein. Interestingly, the absence of GTP dramatically affects the PDE activity of the E1038A/D1039A double mutant, being ~5 folds lower than the wild-type. These kinetic data suggest that this double mutation shifts the OFF→ON equilibrium toward the OFF state, in the absence of GTP. These results clearly show that Glu1038 and Asp1039 residues are involved in stabilizing the protein in the ON state, probably via their interaction with Arg980.

Indeed, Arg980 residue loses its contact(s) in the ON conformation in the double mutant but it can still stabilize the OFF state, explaining the reduced activity of the E1038A/D1039A double mutant in the absence of GTP.

4.7 RmcA contains a LOV domain. Since RmcA is a complex multidomain hybrid protein, we tested if the presence of the upstream domain could affect the kinetic properties and the allosteric control assessed on DUAL conctruct. For this reason, a construct named LOV-DUAL, encoding the LOV-GGDEF-EAL domains, was cloned, expressed and purified. Preliminary catalytic experiments performed using this construct confirmed the presence of the PDE activity and the absence of the DGC one. In addition, this construct exhibits the GTP-dependent allosteric regulation of phosphodiesterase activity. Interestingly, LOV-DUAL showed an higher phosphodiesterase activity, in both presence and absence of GTP, with respect to DUAL protein. The basal DUAL enzyme rate is 0.09 μM/min with respect to 0.15 μM/min of LOV-DUAL. On the other hand, when GTP acts as allosteric regulation the DUAL rate is 0.35 μM/min in contrast to 1.67 μM/min observed with LOV-DUAL construct. These data confirm the presence of a different profile of GTP allosteric regulation between the two constructs: in contrast to the DUAL construct, the GTP positive effect on LOV-DUAL phospodiesterase activity is significantly higher (~11 fold GTP-mediated enhancement in contrast to ~3.9 fold enahcement shown by DUAL construct).
At the same time, a bioinformatic analysis, performed by Prof. Paiardini, suggested that this additional upstream domain, comprising residues 677-795, can be classified as a specialized PAS domain named Light, Oxygen or Voltage (LOV) (Fig. 10). Proteins bearing LOV domains are involved in a large variety of signaling pathways in both prokaryotes and eukaryotes (Taylor and Zhulin, 1999). More in general, Per-ARNT-Sim (PAS) domain superfamily is involved in several signalling pathways sensing different stimuli including oxygen gradient, light, metals availability and cellular redox state (Becker et al., 2011). To fulfill the redox-related biological functions, PAS domain were found to bind heme and flavins. The core structure of the LOV domain is composed of a five-stranded antiparallel β-sheet, surrounded by three short α-helices and several solvent-exposed loops: this structural arrangement generates a module forming a symmetric dimer with the other LOV domain

of the adjacent subunit. In addition, in the inner part of a LOV domain there is an hydrophobic pocket, required for the binding of several organics ligands. LOV domains are well known to bind flavin cofactors, including FMN or FAD, to sense light, redox state or voltage modifications, in order to regulate the activity of the adjacent domains (Fig. 26A); in these domains, the key residue involved in the binding of the FAD cofactor is the asparagine within the NRRK motif. According to this *in silico* analysis, the RmcA region comprising residues 677-795 shows structural homology to different proteins containing LOV domains, including the FAD-containing PAS domain of the NifL from *Azotobacter vinelandiia* (PDB code 2GJ3, sequence identity: 41%) and the redox sensor domain of MmoS from *Methylococcus capsulatus* (PDB code 3EWK, sequence identity: 33%). Moreover, the NRRK motif involved in flavin binding is evolutionarily well conserved in RmcA (residues 760-764) (Fig. 26B).

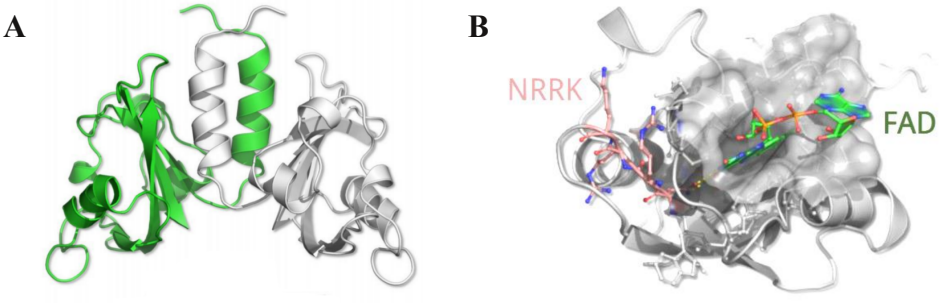

Figure 26. Homology model of RmcA LOV domain. (A) Three dimensional structure of a dimeric LOV domains. (B) Structural model of a FAD moiety inside the hydrophobic pocket of the LOV domain. The NRRK signature is known to be involved in FAD binding interacting with flavin moiety.

4.8 RmcA LOV domain binds FAD. Bioinformatic structural analysis suggested that RmcA LOV domain could bind flavin cofactors; to probe this hypothesis, we performed a reconstitution experiment using FAD the LOV-DUAL construct. As expected, specific FAD binding by the LOV domain of this RmcA construct was observed (Fig. 27A).

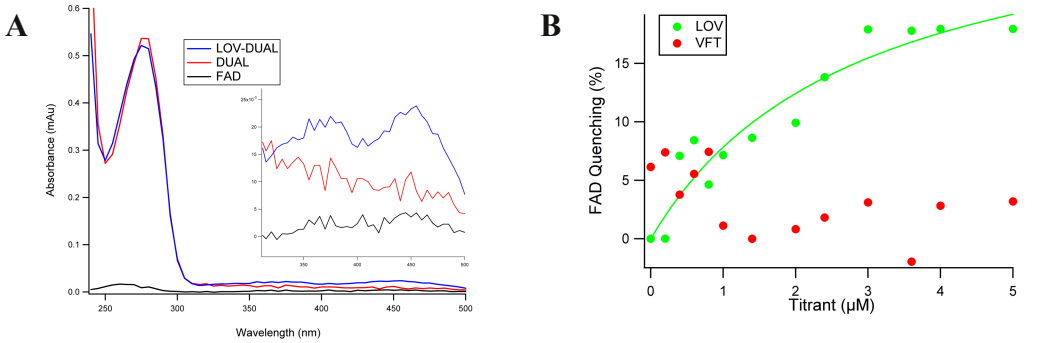

Figure 27. Preliminary evidences of the LOV-FAD interaction. (A) Reconstitution experiments suggested a physical interaction between the LOV domain and FAD molecule. After an incubation of LOV-DUAL and DUAL constructs with excess of FAD for 120' at room temperature, a size exclusion chromatography was performed to eliminate the unbound ligand. In the inset, absorption spectra indicated that only the LOV-DUAL construct retained the FAD molecule, as shown by the double absorbance peak at 350 and 450 nm. (B) FAD Fluorescence Quenching assay was performed by titrating 0.5 μM FAD with increased amount of LOV or VFT construct (green and red circles, respectively). FAD emission quenching indicates that LOV domain binds this flavin.

To better describe this binding, we focused on LOV domain only containing construct. Preliminary experiments indicated that LOV protein is dimeric in solution and titration fluorescence experiments were carried out to assess the putative interaction with FAD . In particular we tested the FAD fluorescence quenching upon the addition of increased amounts of LOV construct (Sengupta et al., 2012). As expected, the LOV domain is able to interact with FAD molecule, with a K_D=2.84±1.13 μM, while no quenching effect is observed titrating FAD with VFT construct as negative internal control since it was predicted not to be able to bind nucleotides (Fig. 27B). To study the binding event involving the RmcA LOV domain, the previous titrations were repeated using ITC as experimental platform. LOV domain specifically binds to FAD with a stoichiometry of 0.38 per monomer and a K_d= 1.6 μM (Fig. 28). The binding stoichiometry suggests that one molecule of FAD is bound by a LOV dimer and this experimental data is in agreement with literature on other LOV-containing proteins (Qi et al., 2009). To test the specificity of this interaction, the titration was carried out also with FMN and pyocyanin: the binding is specific since no binding events occured with both molecules (Fig. 28).

The putative binding of pyocyanin to the RmcA LOV domain was tested since this phenazine binds the cytoplasmic portion harboured by the homologous protein in *P. aeruginosa* PA14 strain (Okegbe et al., 2017).

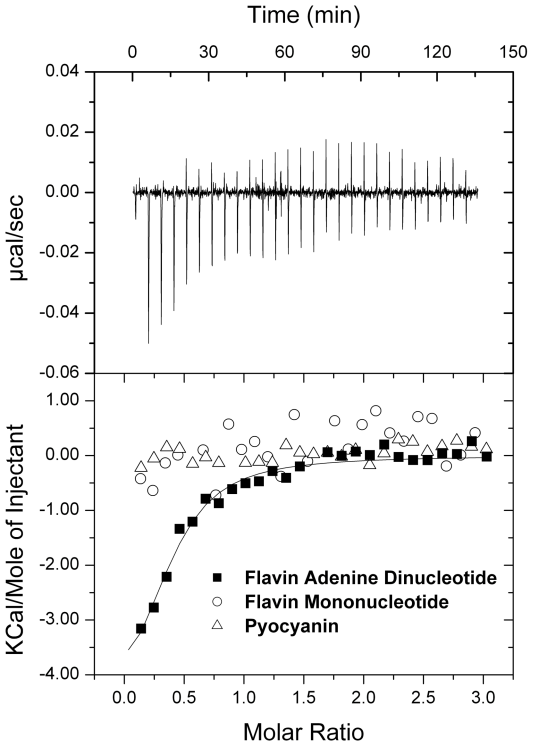

Figure 28. RmcA LOV domain binds FAD. The binding of FAD to LOV was tested by ITC titrating a LOV solution with different amounts of FAD at 25 °C in corrispondent buffer A. In the lower panel the normalized enthalpy exchange (black squares, reported as Kcal/Mol of injectant) has been reported as a function of the Molar Ratio between the injectant and the macromolecule. Data were fitted with the single binding site equation with the Origin software, as provided by the vendor (continuous line), yielding the following parameters: n=0.38±0.05; K_d=1.6±0.9 µM; ΔH=-5.1±0.8 kcal/mol; ΔS=9.34±0.9 cal/mol/deg. To verify the specificity of binding, LOV was titrated with Flavin Mononucleotide and Pyocyanin, as indicate in the figure legend, under the same experimental conditions.

To asses a putative kinetic effect induced by the FAD binding to the LOV domain, we tested the LOV-DUAL PDE catalysis in presence of FAD at different redox state. Indeed, literature data showed that the final output of other LOV/PAS-containing c-di-GMP metabolizing enzymes depends on the redox resting state of the bound flavin which can be O_2-dependent: for instance, the diguanylate cyclase activity of AxDGC2 hybrid protein, from *Acetobacter xylinum*, is increased after the oxidation of FAD bound to its upstream PAS domain, resulting in an higher c-di-GMP production in response to oxygen (Qi et al., 2009). To assess the putative allosteric role of FAD on LOV-DUAL catalysis, we performed a kinetic assay in aerobic as well as under low oxygen tension conditions (obtained by fluxing samples with nitrogen to remove excess oxygen).

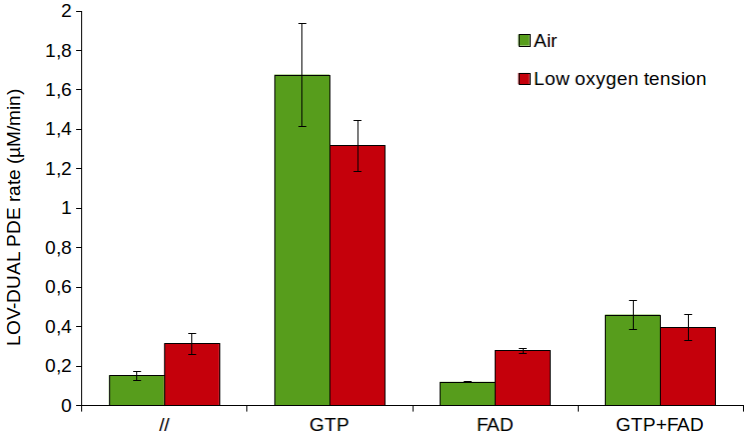

Figure 29. PDE activity of LOV-DUAL is affected by GTP and FAD. Time course assay was performed in both aerobic and anaerobic conditions (panel A and B, respectively). In both conditions, the rate of the enzyme is positively affected by the presence of GTP, as expected. Interestingly, the FAD reduces the extent of the GTP-mediated enhancement. In addition, the basal activity of LOV-DUAL is clearly improved in low oxygen condition.

Despite the confirmed binding between FAD and LOV domain, performing kinetic experiments using FAD, as sole allosteric putative regulator, has no effect on PDE activity under both tested conditions (Fig. 29).

Interestingly, the phosphodiesterase reaction in presence of both GTP and FAD as allosteric regulators leads to a reduced turnover. The FAD-dependent inhibition occurs in both aerobic and anaerobic conditions to a similar extent (~3.6 in aerobic condition and ~3.3 fold in low oxygen environment) (Fig. 29). These data suggest that the FAD cofactor works as an allosteric inhibitor of the GTP-mediated phosphodiesterase enhancement. In agreement with the bioinformatic structural model, FAD specifically binds to the LOV domain of RmcA and this interaction triggers a clear reduction of the phosphodiesterase activity of LOV-DUAL construct only when the latter is bound to the GTP allosteric regulator.

4.10 The GGDEF domain is able to hydrolyse GTP. The concentration of GTP and c-di-GMP is very different and variable within the bacterial cell, in the sub-mM range and in the low μM range, respectively (Christen et al., 2005 ; Simm et al., 2004 ; Weinhouse et al., 1997). Due to the cellular concentration of GTP, the DUAL superdomain of RmcA could be predominantly in the ON state. To assess if DUAL activity may vary according to the different levels of the two nucleotides relative to the protein, we repeated the PDE kinetic assays on DUAL with GTP at higher protein concentration (8 μM DUAL rather than 1 μM, using the buffer optimized for PDE) to evaluate if the GTP effect is unchanged. Under these conditions, the PDE activity is not affected, but a novel chemical species populates, corresponding to GMP as confirmed by mass spectrometry (Fig. 30A). The formation of GMP starts only when c-di-GMP concentration drops below about 8 μM (Fig. 30B) and proceeds at $1.8\pm(0,6)\ x10^{-2}\ min^{-1}$. The unexpected GTPase activity of DUAL starts only when c-di-GMP concentration drops down; thus we tested if this activity occured also at different c-di-GMP concentrations. We performed the same experiment with a low c-di-GMP concentration and without the dinucleotide. Under these conditions, we found that GTP hydrolysis occurs at a greater rate, specifically at $2.3\pm(0.4)\ x10^{-2}\ min^{-1}$ with a low c-di-GMP concentration and at $3.9\pm(0.6)\ x10^{-2}\ min^{-1}$ without c-di-GMP (Fig. 30C). These data suggest that the unexpected GTPase reactivity is negatively affected by the starting amount of c-di-GMP which in turn affects the PDE time course.

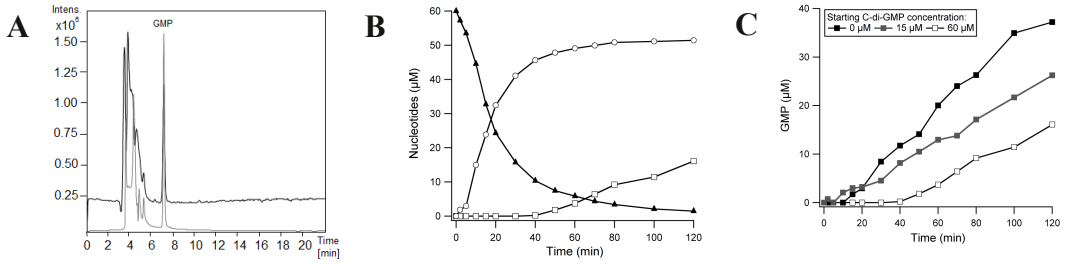

Figure 30. The GTPase activity of DUAL. (A) Characterization of the GTPase activity of DUAL; HPLC-MS chromatogram (black) and HPLC-DAD chromatogram (grey) of the nucletoide content, monitored at 250 nm wavelength, of DUAL reaction mixture. (B) Nucleotides content at different times of the catalytic reaction carried out with 8 µM DUAL in experimental condition optimized for GTPase activity (GMP, squares; c-di-GMP, triangles; pGpG, circles). GTP content has not been reported since its peak overlaps with those of buffer. (C) Time-course of the GTPase reaction performed with 8 µM DUAL, in presence of different amounts of c-di-GMP or in absence of it (as indicated in figure legend), in experimental condition optimized for GTPase activity.

In order to exclude the possibility that this unusual GTPase activity could be due to an experimental artifact associated with the RmcA DUAL construct, we tested the presence of GTPase activity using the LOV-DUAL construct. As expected, also this RmcA-derived construct converts GTP to GMP and this GTPase activity decreases when c-di-GMP is present (Fig. 31). In addition, we observed that products corresponding to pGpG and c-di-GMP accumulate when the enzyme is incubated with GTP as sole substrate. This data indicates that the construct, only under these kinetic experimental conditions, shows a limited diguanylate cyclase activity, producing c-di-GMP *via* the GGDEF domain which is then degraded to pGpG by the EAL one. A possible explanation of this kinetic behaviour is that both the greater amount of LOV-DUAL protein promoted the DGC random competent dimerization of the GGDEF domains likely responsible for the production of c-di-GMP (Fig. 31A).

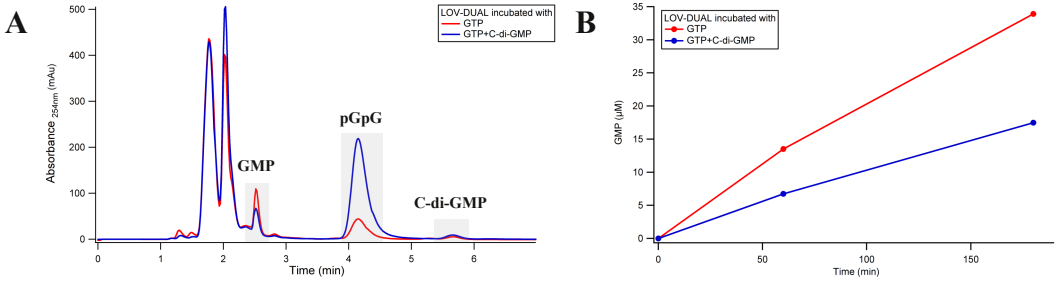

Figure 31. LOV-DUAL shows a GTPase activity. (A) RP-HPLC Chromatograms confirm that 8 μM LOV-DUAL, incubated with GTP as only substrate, produces GMP. The GTPase activity occurs also when the enzyme is incubated with both GTP and c-di-GMP. In addition, LOV-DUAL converts GTP to c-di-GMP showing a DGC activity which is absent in the DUAL construct. (B) Time-course of GTPase activity performed with 8 μM LOV-DUAL, GTP and with or without c-di-GMP (blu and red line, respectively), in experimental conditions optimized for GTPase catalysis.

To investigate the main properties of the GTPase activity, different experiments were performed. Since GMP can be produced from pGpG by a PDE-B activity (Stelitano et al., 2013), we performed a kinetic assay incubating the DUAL protein with excess of GTP and pGpG as only substrate. GMP product accumulates only when the protein is incubated with GTP as starting substrate (Fig. 32A), indicating that the GMP is not produced by a PDE-B activity. To assess which domain was responsible of the conversion of GTP to GMP, we tested the GTPase activity using the both DUAL and EAL-2 constructs: incubating both enzymes with GTP, we observed that only the DUAL construct is competent for the GTPase activity, indicating that GGDEF domain is the key domain involved in this unexpected catalysis (Fig. 32B). In agreement with this result, the GGDEF mutant (DUAL E890A), despite its sub-μM affinity for GTP, is unable to convert this nucleotide in GMP, likely because the Glu890 residue is also involved in GTP hydrolysis (Fig. 32B). In addition, we observed that the GTPase activity required either Mg^{2+} or Mn^{2+} while it is abolished by the presence of other bivalent cations, including Zn^{2+} and Ca^{2+} (Fig. 32C).

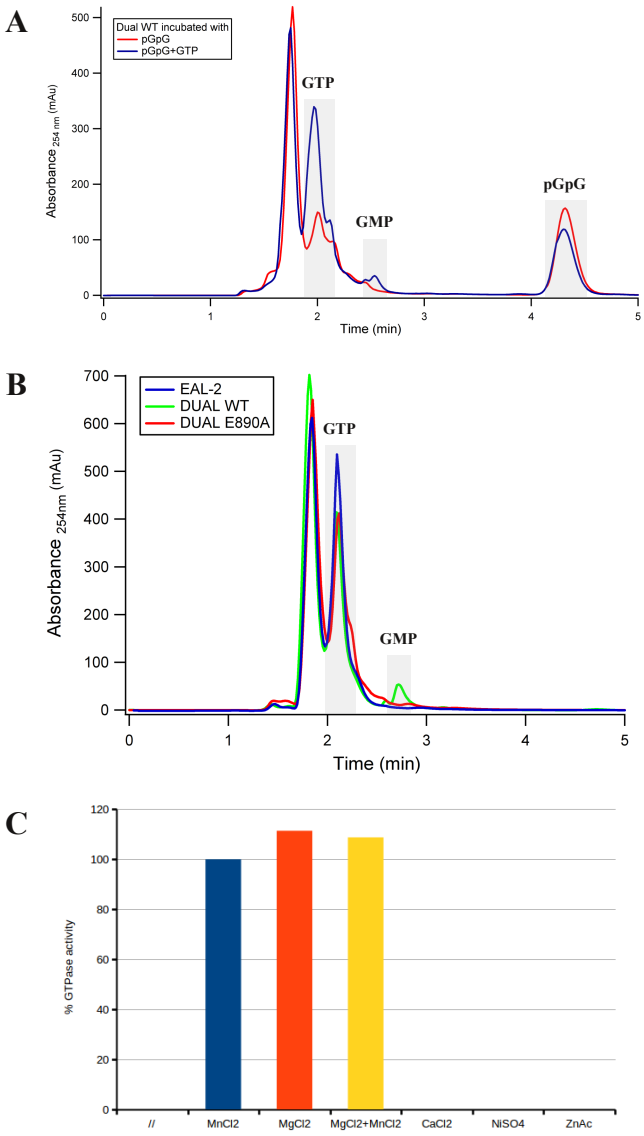

Figure 32. Properties of GTPase activity. (A) HPLC-RP chromatograms revealed that the GMP is specifically produced starting from GTP (blue line) as substrate since no GMP accumulates when

pGpG is used as substrate (red line). This indicates that GMP is not produced by a PDE-b activity of DUAL construct. (B) HPLC-RP chromatograms indicates that the GGDEF domain of DUAL is responsible for the production of GMP (green line) since EAL-2 construct is unable to degrade GTP (red line) and that no GMP accumulates when GGDEF signature is mutated (E890A) (blue line). (C) GTPase reaction was performed incubating 10 μM DUAL in a reaction solution optimized for GTPase catalysis containing different divalent ions: the GGDEF domain requires either Mn^{2+} or Mg^{2+} or both (blue, orange and yellow bar, respectively) for its GTPase activity.

4.11 GGDEF uncompetent dimerization promotes GMP production. If this background reactivity is a general feature of the GGDEF domains, it could bias kinetic studies describing GGDEF-containing proteins; therefore the establishment of the proper kinetic conditions is required for rigorous studies of this versatile domain. In order to deeply establish the kinetic property of this domain, we focused our attention on several GGDEF containing enzymes. The GTPase activity of DUAL could be ascribed to an intrinsic reactivity of the 'monomeric' GGDEF domain since the physiological DGC reaction requires not only the dimerization of the GGDEF domains but also the facing of the two active sites in order to produce c-di-GMP starting from two molecules of GTP. In order to assess if the oligomeric state of GGDEF domains could be involved in GTPase activity, we probed the presence of this reactivity on two different DGCs: PleD from *C. crescentus* and the GGDEF containing portion of YfiN, from *P. aeruginosa*, an inactive truncated version purified as monomer.

The diguanylate cyclase activity of PleD requires the dimerization of GGDEF domains and this conformational process can be induced *in vitro* by adding the chemical activator beryllium fluoride (Fernicola et al., 2016). To test the possibility that GGDEF shows GTPase activity when the physiological diguanylate cyclase can not occur, we performed the kinetic assay with and without this activator. As expected, during its diguanylate cyclase activity PleD, c-di-GMP accumulates while no GMP production is detected (Fig. 33A and 33B). In agreement with our hypothesis, when the productive dimerization of the GGDEF domains, necessary for the DGC activity of PleD, was inhibited by the absence of $BeCl_2$, GMP accumulates from GTP while no significant c-di-GMP production is observed (Fig. 33A and 33B). To confirm that an incompetent GGDEF domain can show an unusual GTPase activity, we tested the GGDEF containing construct of YfiN inactive as diguanylate cyclase because this monomeric form is unable to dimerize during

turnover (Giardina et al., 2013). As expected, the kinetic data clearly shows that the inactive GGDEF domain of YfiN starts accumulating GMP without any production of c-di-GMP (Fig. 33C and 33D). These results indicate that the GGDEF domain shows a unusual GTPase activity occurring when the main physiological DGC activity cannot take place due to the inhability to form the active dimer caused by allosteric constrains, as in PleD, or domain truncation, as in YfiN.

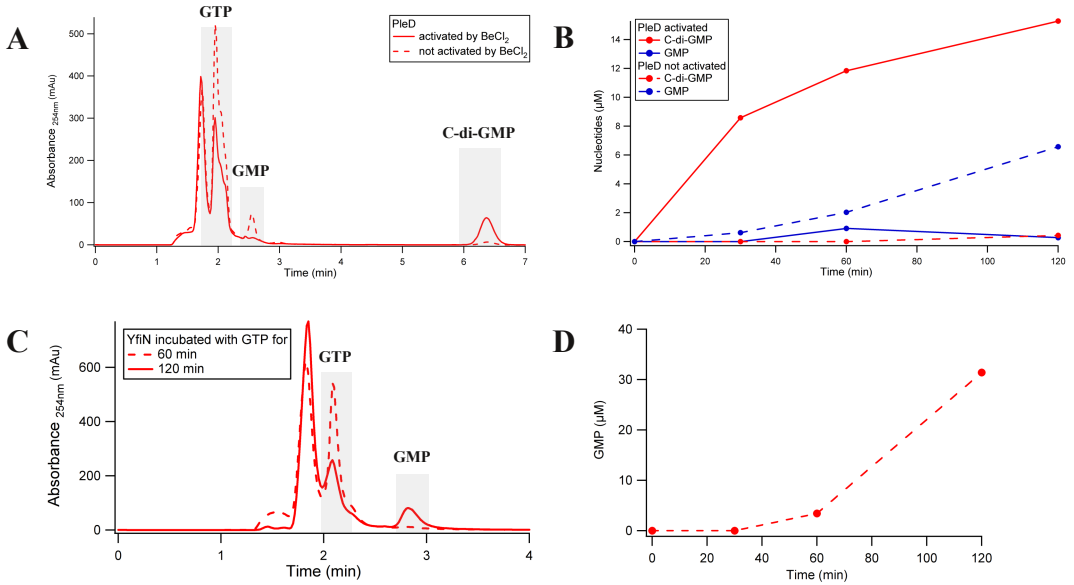

Figure 33. The GGDEF domain of other DGCs is able to produce GMP. (A) HPLC-RP chromatograms of PleD-mediated diguanylate cyclase reaction. Catalytic reaction was carried out either using PleD enzyme activated as DGC by $BeCl_2$ (continuous lines) or with the inactivated form of the enzyme, which was obtained by not adding $BeCl_2$ (dotted lines). (B) Time course of both PleD DGC and GTPase activities (red and blue lines, respectively). (C) HPLC-RP chromatograms of YfiN GTPase activity. In particular the GTPase activity of YfiN shows a clear lag-phase starting to accumulate GMP after 60 minutes (continuous red line). (D) Time course of YfiN GTPase reaction. Aliquots of the reaction were stop at different times (30-60-120 minutes) and they were analyzed as described above in Materials and Methods chapter.

CONCLUSIONS

In the last years, the importance of the bacterial second messenger c-di-GMP as key player regulating biofilm formation and dispersal raised up. The large number of groups currently studying this messenger allowed to unveil the general properties of enzymes, receptors and effectors involved in c-di-GMP signalling. However, few biochemical data describing the role of the GGDEF-EAL hybrid proteins in c-di-GMP homeostasis are available. In addition, few biological data describing how environmental signals control the enzymes involved in the c-di-GMP network itself are available.

The aim of my PhD was to biochemically characterize a member of GGDEF-EAL hybrid protein with a putative environmental sensor domain in order to both identify the signalling molecule as well as to describe the final output of this enzyme. This study has been carried out focusing on the product of the gene *RmcA* from *Pseudomonas aeruginosa*, a multidomain protein composed by a periplasmic sensory domain, a transmembrane helix, three Per-Arnt-Sim (PAS) domain and one light, oxygen, or voltage domain (LOV) and finally the GGDEF-EAL catalytic module. Preliminary bioinformatic structural analysis, carried out by Prof. Paiardini, suggested that this RmcA could sense the amino acid L-arginine by its N-terminal sensor domain folding as a VFT domain. In agreement with this bioinformatic prediction, our results reveal that RmcA VFT domain specifically binds this nutrients and this interaction triggers an *in vivo* effect by lowering c-di-GMP levels. Interestingly, analysis of RmcA homologous sequences indicated that this domain organization is observed only in *Pseudomonas* genus belonging bacteria (data not shown). L-arginine is a versatile metabolite acting as a source of carbon, energy, and nitrogen since *P. aeruginosa* metabolizes this amino acid via several enzymes such as arginine decarboxylase (ADC), dehydrogenase (ADH), succinyl-transferase (AST, aerobic conditions). In anaerobic condition, the bacterium utilizes this amino acid by the arginine deiminase pathway (ADI) producing ATP (Lu et al., 2004): the arginine fermentation allows the bacterium to survive when denitrification does not occur (Kuroki et al., 2014). Further biochemical and microbiological studies aimed to assess the molecular mechanism through which the L-arginine binding is

propagated to the GGDEF-EAL effector domains in RmcA are required. However these findings describe a novel link between L-arginine metabolism and c-di-GMP signalling on *P. aeruginosa*. Both *in vivo* and the preliminary enzymatic assay on the full length RmcA protein indicated that this protein works as a phosphodiesterase. Focusing on the GGDEF-EAL containing region of RmcA, we confirmed the EAL-dependent phosphodiesterase activity. In addition, we found that a cross-talk between GGDEF and EAL domains occurs. The GGDEF domain negatively controls the EAL activity; GTP binding to GGDEF domain releases this negative inter-domain cross-talk through a large conformational change resulting in the EAL-EAL dimerization. This is not the first experimental evidence of the role of GTP as allosteric regulator of EAL activity via the GGDEF domain (An et al., 2010 ; Christen et al., 2006). It is important to consider that both GTP and c-di-GMP nucleotides are key players in bacterial physiology since GTP controls the cell's metabolic status while c-di-GMP regulates the planktonic/sessile transition: given that their metabolic pathways are tightly interconnected, a mutual control is strategic for bacteria. Within the bacterial cell, the levels of GTP and c-di-GMP are very different, in the sub-mM and low μM range, respectively (Christen et al., 2005 ; Weinhouse et al., 1997 ; Simm et al., 2004). Our *in vitro* kinetic results indicated that GTP triggers the maximal PDE activity in the micromolar range which is much smaller than the millimolar range of GTP levels in bacterial cells: in this scenario the RmcA GGDEF domain would always be fully occupied by GTP, blocking the regulatory model described above. However, this discrepancy could be explained by the possible *in vivo* regulating roles of the upstream domains, missing in the DUAL construct of RmcA. To follow this hypothesis, we preliminary described the RmcA LOV domain. Indeed, in addition to the signal transduction mediated by L-arginine through the VFT moiety, domain architecture analysis indicates that RmcA contains a Light, Oxygen or Voltage (LOV) domain, belonging to the PAS superfamily, upstream the GGDEF-EAL region. LOV domains are known to bind flavin cofactor (FMN or FAD) to perceive light, redox or voltage modifications, in order to control the activity of their adjacent domains. We confirmed the binding of the RmcA LOV domain to the FAD molecule, and showed that this interaction triggers, *in vitro*, a kinetic effect on the downstream catalytic region regardless the oxygen availability.

Indeed, experimental data suggests that FAD works as an allosteric inhibitor of the GTP-dependent enhancement of the LOV-DUAL phosphodiesterase activity and thus further biochemical studies will be required to understand the molecular mechanism behind this inhibition. In particular, there is the possibility that, under our kinetic setup, different FAD redox states are not fully populated, suggesting that kinetic characterization of LOV-DUAL construct will have to be carried out in the presence of redox agents. In addition, structural experiments will be carried out in order to assess if FAD molecule controls the accessibility of GTP to GGDEF binding site, thus showing an upstram regulation of the GGDEF domain. All these results describe a multi-level regulation controlling the activity of RmcA hybrid protein: this enzyme senses both the environmental state (i.e nutrients availability) and the cellular state (redox power and energetic state) finely tuning the c-di-GMP metabolism.

Additional important finding emerged from these studies: a novel unusual GTPase activity GGDEF-mediated was kinetically described. This kinetic property was observed in GGDEF domains belonging to DGCs and RmcA hybrid protein: in DGCs this side effect activity takes place when the main diguanylate cyclase activity does not occur while in the tested hybrid protein the GTPase activity seems to compete with the PDE one, overcoming it when the c-di-GMP concentration drops down. Regardless the biological relevance of this unusual GGDEF dependent GTPase activity, it is important to consider the latter one when performing the biochemical characterization of the GGDEF containing enzymes.

REFERENCES

Antoniani, D., Rossi, E., Rinaldo, S., Bocci, P., Lolicato, M., Paiardini, A., Raffaelli, N., Cutruzzolà, F., and Landini, P. (2013). The immunosuppressive drug azathioprine inhibits biosynthesis of the bacterial signal molecule cyclic-di-GMP by interfering with intracellular nucleotide pool availability. Appl Microbiol Biotechnol 97, 7325-7336.

Barbier, M., Damron, F.H., Bielecki, P., Suárez-Diez, M., Puchałka, J., Albertí, S., Dos Santos, V.M., and Goldberg, J.B. (2014). From the environment to the host: re-wiring of the transcriptome of Pseudomonas aeruginosa from 22°C to 37°C. PLoS One 9, e89941.

Basu Roy, A., and Sauer, K. (2014). Diguanylate cyclase NicD-based signalling mechanism of nutrient-induced dispersion by Pseudomonas aeruginosa. Mol Microbiol 94, 771-793.

Becker, D.F., Zhu, W., and Moxley, M.A. (2011). Flavin redox switching of protein functions. Antioxid Redox Signal 14, 1079-1091.

Bellini, D., Caly, D.L., McCarthy, Y., Bumann, M., An, S.Q., Dow, J.M., Ryan, R.P., and Walsh, M.A. (2014). Crystal structure of an HD-GYP domain cyclic-di-GMP phosphodiesterase reveals an enzyme with a novel trinuclear catalytic iron centre. Mol Microbiol 91, 26-38.

Bhinu, V.S. (2005). Insight into biofilm-associated microbial life. J Mol Microbiol Biotechnol 10, 15-21.

Bobrov, A.G., Kirillina, O., Forman, S., Mack, D., and Perry, R.D. (2008). Insights into Yersinia pestis biofilm development: topology and co-interaction of Hms inner membrane proteins involved in exopolysaccharide production. Environ Microbiol 10, 1419-1432.

Cashel, M., and Gallant, J. (1969). Two compounds implicated in the function of the RC gene of Escherichia coli. Nature 221, 838-841.

Chambers, J.R., Liao, J., Schurr, M.J., and Sauer, K. (2014). BrlR from Pseudomonas aeruginosa is a c-di-GMP-responsive transcription factor. Mol Microbiol 92, 471-487.

Chan, C., Paul, R., Samoray, D., Amiot, N.C., Giese, B., Jenal, U., and Schirmer, T. (2004). Structural basis of activity and allosteric control of diguanylate cyclase. Proc Natl Acad Sci U S A 101, 17084-17089.

Chang, A.L., Tuckerman, J.R., Gonzalez, G., Mayer, R., Weinhouse, H., Volman, G., Amikam, D., Benziman, M., and Gilles-Gonzalez, M.A. (2001). Phosphodiesterase A1, a regulator of cellulose synthesis in Acetobacter xylinum, is a heme-based sensor. Biochemistry 40, 3420-3426.

Chen, W., Kuolee, R., and Yan, H. (2010). The potential of 3',5'-cyclic diguanylic acid (c-di-GMP) as an effective vaccine adjuvant. Vaccine 28, 3080-3085.

Chen, Z.H., and Schaap, P. (2012). The prokaryote messenger c-di-GMP triggers stalk cell differentiation in Dictyostelium. Nature 488, 680-683.

Christen, M., Christen, B., Folcher, M., Schauerte, A., and Jenal, U. (2005). Identification and characterization of a cyclic di-GMP-specific phosphodiesterase and its allosteric control by GTP. J Biol Chem 280, 30829-30837.

Christen, M., Kulasekara, H.D., Christen, B., Kulasekara, B.R., Hoffman, L.R., and Miller, S.I. (2010). Asymmetrical distribution of the second messenger c-di-GMP upon bacterial cell division. Science 328, 1295-1297.

Clifton, B.E., and Jackson, C.J. (2016). Ancestral Protein Reconstruction Yields Insights into Adaptive Evolution of Binding Specificity in Solute-Binding Proteins. Cell Chem Biol 23, 236-245.

Conner, J.G., Zamorano-Sánchez, D., Park, J.H., Sondermann, H., and Yildiz, F.H. (2017). The ins and outs of cyclic di-GMP signaling in Vibrio cholerae. Curr Opin Microbiol 36, 20-29.

Cooley, R.B., O'Donnell, J.P., and Sondermann, H. (2016). Coincidence detection and bi-directional transmembrane signaling control a bacterial second messenger receptor. Elife 5.

Cutruzzolà, F., and Frankenberg-Dinkel, N. (2016). Origin and Impact of Nitric Oxide in Pseudomonas aeruginosa Biofilms. J Bacteriol 198, 55-65.

Dahlstrom, K.M., Collins, A.J., Doing, G., Taroni, J.N., Gauvin, T.J., Greene, C.S., Hogan, D.A., and O'Toole, G.A. (2018). A Multimodal Strategy Used by a Large c-di-GMP Network. J Bacteriol 200

Dahlstrom, K.M., Giglio, K.M., Collins, A.J., Sondermann, H., and O'Toole, G.A. (2015). Contribution of Physical Interactions to Signaling Specificity between a Diguanylate Cyclase and Its Effector. MBio 6, e01978-01915.
Davies, D. (2003). Understanding biofilm resistance to antibacterial agents. Nat Rev Drug Discov 2, 114-122.
Deng, Y., Schmid, N., Wang, C., Wang, J., Pessi, G., Wu, D., Lee, J., Aguilar, C., Ahrens, C.H., Chang, C., et al. (2012). Cis-2-dodecenoic acid receptor RpfR links quorum-sensing signal perception with regulation of virulence through cyclic dimeric guanosine monophosphate turnover. Proc Natl Acad Sci U S A 109, 15479-15484.
Duerig, A., Abel, S., Folcher, M., Nicollier, M., Schwede, T., Amiot, N., Giese, B., and Jenal, U. (2009). Second messenger-mediated spatiotemporal control of protein degradation regulates bacterial cell cycle progression. Genes Dev 23, 93-104.
Fernicola, S., Paiardini, A., Giardina, G., Rampioni, G., Leoni, L., Cutruzzolà, F., and Rinaldo, S. (2016). In Silico Discovery and In Vitro Validation of Catechol-Containing Sulfonohydrazide Compounds as Potent Inhibitors of the Diguanylate Cyclase PleD. J Bacteriol 198, 147-156.
Galperin, M.Y. (2005). A census of membrane-bound and intracellular signal transduction proteins in bacteria: bacterial IQ, extroverts and introverts. BMC Microbiol 5, 35.
Giardina, G., Paiardini, A., Fernicola, S., Franceschini, S., Rinaldo, S., Stelitano, V., and Cutruzzolà, F. (2013). Investigating the allosteric regulation of YfiN from Pseudomonas aeruginosa: clues from the structure of the catalytic domain. PLoS One 8, e81324.
Gibson, R.L., Burns, J.L., and Ramsey, B.W. (2003). Pathophysiology and management of pulmonary infections in cystic fibrosis. Am J Respir Crit Care Med 168, 918-951.
Goforth, J.B., Walter, N.E., and Karatan, E. (2013). Effects of polyamines on Vibrio cholerae virulence properties. PLoS One 8, e60765.
Ha, D.G., Merritt, J.H., Hampton, T.H., Hodgkinson, J.T., Janecek, M., Spring, D.R., Welch, M., and O'Toole, G.A. (2011). 2-Heptyl-4-quinolone, a precursor of the Pseudomonas quinolone signal molecule, modulates swarming motility in Pseudomonas aeruginosa. J Bacteriol 193, 6770-6780.

Ha, D.G., and O'Toole, G.A. (2015). c-di-GMP and its Effects on Biofilm Formation and Dispersion: a Pseudomonas Aeruginosa Review. Microbiol Spectr 3, MB-0003-2014.
Hay, I.D., Remminghorst, U., and Rehm, B.H. (2009). MucR, a novel membrane-associated regulator of alginate biosynthesis in Pseudomonas aeruginosa. Appl Environ Microbiol 75, 1110-1120.
Hecht, G.B., and Newton, A. (1995). Identification of a novel response regulator required for the swarmer-to-stalked-cell transition in Caulobacter crescentus. J Bacteriol 177, 6223-6229.
Hengge, R. (2016). Trigger phosphodiesterases as a novel class of c-di-GMP effector proteins. Philos Trans R Soc Lond B Biol Sci 371.
Henry, J.T., and Crosson, S. (2011). Ligand-binding PAS domains in a genomic, cellular, and structural context. Annu Rev Microbiol 65, 261-286.
Herrmann, G., Yang, L., Wu, H., Song, Z., Wang, H., Høiby, N., Ulrich, M., Molin, S., Riethmüller, J., and Döring, G. (2010). Colistin-tobramycin combinations are superior to monotherapy concerning the killing of biofilm Pseudomonas aeruginosa. J Infect Dis 202, 1585-1592.
Hickman, J.W., and Harwood, C.S. (2008). Identification of FleQ from Pseudomonas aeruginosa as a c-di-GMP-responsive transcription factor. Mol Microbiol 69, 376-389.
Inuzuka, S., Kakizawa, H., Nishimura, K.I., Naito, T., Miyazaki, K., Furuta, H., Matsumura, S., and Ikawa, Y. (2018). Recognition of cyclic-di-GMP by a riboswitch conducts translational repression through masking the ribosome-binding site distant from the aptamer domain. Genes Cells 23, 435-447.
Jakobsen, T.H., Tolker-Nielsen, T., and Givskov, M. (2017). Bacterial Biofilm Control by Perturbation of Bacterial Signaling Processes. Int J Mol Sci 18.
Jenal, U., Reinders, A., and Lori, C. (2017). Cyclic di-GMP: second messenger extraordinaire. Nat Rev Microbiol 15, 271-284.
Karaolis, D.K., Means, T.K., Yang, D., Takahashi, M., Yoshimura, T., Muraille, E., Philpott, D., Schroeder, J.T., Hyodo, M., Hayakawa, Y., et al. (2007). Bacterial c-di-GMP is an immunostimulatory molecule. J Immunol 178, 2171-2181.
Karatan, E., and Watnick, P. (2009). Signals, regulatory networks, and materials that build and break bacterial biofilms. Microbiol Mol Biol Rev 73, 310-347.

Kato, K., Ishii, R., Hirano, S., Ishitani, R., and Nureki, O. (2015). Structural Basis for the Catalytic Mechanism of DncV, Bacterial Homolog of Cyclic GMP-AMP Synthase. Structure 23, 843-850.
Krasteva, P.V., Fong, J.C., Shikuma, N.J., Beyhan, S., Navarro, M.V., Yildiz, F.H., and Sondermann, H. (2010). Vibrio cholerae VpsT regulates matrix production and motility by directly sensing cyclic di-GMP. Science 327, 866-868.
Kulasekara, H.D., Ventre, I., Kulasekara, B.R., Lazdunski, A., Filloux, A., and Lory, S. (2005). A novel two-component system controls the expression of Pseudomonas aeruginosa fimbrial cup genes. Mol Microbiol 55, 368-380.
Landini, P. (2009). Cross-talk mechanisms in biofilm formation and responses to environmental and physiological stress in Escherichia coli. Res Microbiol 160, 259-266.
Lindenberg, S., Klauck, G., Pesavento, C., Klauck, E., and Hengge, R. (2013). The EAL domain protein YciR acts as a trigger enzyme in a c-di-GMP signalling cascade in E. coli biofilm control. EMBO J 32, 2001-2014.
Liu, K., Bittner, A.N., and Wang, J.D. (2015). Diversity in (p)ppGpp metabolism and effectors. Curr Opin Microbiol 24, 72-79.
Lovering, A.L., Capeness, M.J., Lambert, C., Hobley, L., and Sockett, R.E. (2011). The structure of an unconventional HD-GYP protein from Bdellovibrio reveals the roles of conserved residues in this class of cyclic-di-GMP phosphodiesterases. MBio 2.
Lu, C.D., Yang, Z., and Li, W. (2004). Transcriptome analysis of the ArgR regulon in Pseudomonas aeruginosa. J Bacteriol 186, 3855-3861.
Mantoni, F., Paiardini, A., Brunotti, P., D'Angelo, C., Cervoni, L., Paone, A., Cappellacci, L., Petrelli, R., Ricciutelli, M., Leoni, L., et al. (2018). Insights into the GTP-dependent allosteric control of c-di-GMP hydrolysis from the crystal structure of PA0575 protein from Pseudomonas aeruginosa. FEBS J.
Matsuyama, B.Y., Krasteva, P.V., Baraquet, C., Harwood, C.S., Sondermann, H., and Navarro, M.V. (2016). Mechanistic insights into c-di-GMP-dependent control of the biofilm regulator FleQ from Pseudomonas aeruginosa. Proc Natl Acad Sci U S A 113, E209-218.
Mills, E., Petersen, E., Kulasekara, B.R., and Miller, S.I. (2015). A direct screen for c-di-GMP modulators reveals a Salmonella Typhimurium periplasmic

L-arginine-sensing pathway. Sci Signal 8, ra57.
Monds, R.D., Newell, P.D., Gross, R.H., and O'Toole, G.A. (2007). Phosphate-dependent modulation of c-di-GMP levels regulates Pseudomonas fluorescens Pf0-1 biofilm formation by controlling secretion of the adhesin LapA. Mol Microbiol 63, 656-679.
Moskowitz, S.M., and Ernst, R.K. (2010). The role of Pseudomonas lipopolysaccharide in cystic fibrosis airway infection. Subcell Biochem 53, 241-253.
Navarro, M.V., Newell, P.D., Krasteva, P.V., Chatterjee, D., Madden, D.R., O'Toole, G.A., and Sondermann, H. (2011). Structural basis for c-di-GMP-mediated inside-out signaling controlling periplasmic proteolysis. PLoS Biol 9, e1000588.
Newell, P.D., Monds, R.D., and O'Toole, G.A. (2009). LapD is a bis-(3',5')-cyclic dimeric GMP-binding protein that regulates surface attachment by Pseudomonas fluorescens Pf0-1. Proc Natl Acad Sci U S A 106, 3461-3466.
Okegbe, C., Fields, B.L., Cole, S.J., Beierschmitt, C., Morgan, C.J., Price-Whelan, A., Stewart, R.C., Lee, V.T., and Dietrich, L.E.P. (2017). Electron-shuttling antibiotics structure bacterial communities by modulating cellular levels of c-di-GMP. Proc Natl Acad Sci U S A 114, E5236-E5245.
Orr, M.W., Donaldson, G.P., Severin, G.B., Wang, J., Sintim, H.O., Waters, C.M., and Lee, V.T. (2015). Oligoribonuclease is the primary degradative enzyme for pGpG in Pseudomonas aeruginosa that is required for cyclic-di-GMP turnover. Proc Natl Acad Sci U S A 112, E5048-5057.
Paiardini, A., Mantoni, F., Giardina, G., Paone, A., Janson, G., Leoni, L., Rampioni, G., Cutruzzolà, F., and Rinaldo, S. (2018). A novel bacterial L-arginine sensor controlling c-di-GMP levels in Pseudomonas aeruginosa. Proteins.
Paul, R., Weiser, S., Amiot, N.C., Chan, C., Schirmer, T., Giese, B., and Jenal, U. (2004). Cell cycle-dependent dynamic localization of a bacterial response regulator with a novel di-guanylate cyclase output domain. Genes Dev 18, 715-727.
Pawar, S.V., Messina, M., Rinaldo, S., Cutruzzolà, F., Kaever, V., Rampioni, G., and Leoni, L. (2016). Novel genetic tools to tackle c-di-GMP-dependent signalling in Pseudomonas aeruginosa. J Appl Microbiol 120, 205-217.
Peng, J., Cao, J., Ng, F.M., and Hill, J. (2017). Pseudomonas aeruginosa develops Ciprofloxacin resistance from low to high level with distinctive proteome changes. J Proteomics 152, 75-87.

Phippen, C.W., Mikolajek, H., Schlaefli, H.G., Keevil, C.W., Webb, J.S., and Tews, I. (2014). Formation and dimerization of the phosphodiesterase active site of the Pseudomonas aeruginosa MorA, a bi-functional c-di-GMP regulator. FEBS Lett 588, 4631-4636.
Pultz, I.S., Christen, M., Kulasekara, H.D., Kennard, A., Kulasekara, B., and Miller, S.I. (2012). The response threshold of Salmonella PilZ domain proteins is determined by their binding affinities for c-di-GMP. Mol Microbiol 86, 1424-1440.
Qi, Y., Rao, F., Luo, Z., and Liang, Z.X. (2009). A flavin cofactor-binding PAS domain regulates c-di-GMP synthesis in AxDGC2 from Acetobacter xylinum. Biochemistry 48, 10275-10285.
Rinaldo, S., Giardina, G., Mantoni, F., Paone, A., and Cutruzzolà, F. (2018). Beyond nitrogen metabolism: nitric oxide, cyclic-di-GMP and bacterial biofilms. FEMS Microbiol Lett 365.
Rinaldo, S., Paiardini, A., Stelitano, V., Brunotti, P., Cervoni, L., Fernicola, S., Protano, C., Vitali, M., Cutruzzolà, F., and Giardina, G. (2015). Structural basis of functional diversification of the HD-GYP domain revealed by the Pseudomonas aeruginosa PA4781 protein, which displays an unselective bimetallic binding site. J Bacteriol 197, 1525-1535.
Rochex, A., and Lebeault, J.M. (2007). Effects of nutrients on biofilm formation and detachment of a Pseudomonas putida strain isolated from a paper machine. Water Res 41, 2885-2892.
Ross, P., Weinhouse, H., Aloni, Y., Michaeli, D., Weinberger-Ohana, P., Mayer, R., Braun, S., de Vroom, E., van der Marel, G.A., van Boom, J.H., et al. (1987). Regulation of cellulose synthesis in Acetobacter xylinum by cyclic diguanylic acid. Nature 325, 279-281.
Rybtke, M., Hultqvist, L.D., Givskov, M., and Tolker-Nielsen, T. (2015). Pseudomonas aeruginosa Biofilm Infections: Community Structure, Antimicrobial Tolerance and Immune Response. J Mol Biol 427, 3628-3645.
Römling, U. (2012). Cyclic di-GMP, an established secondary messenger still speeding up. Environ Microbiol 14, 1817-1829.
Römling, U. (2015). Small molecules with big effects: Cyclic di-GMP-mediated stimulation of cellulose production by the amino acid L-arginine. Sci Signal 8, fs12.

Römling, U., and Balsalobre, C. (2012). Biofilm infections, their resilience to therapy and innovative treatment strategies. J Intern Med 272, 541-561.
Römling, U., Galperin, M.Y., and Gomelsky, M. (2013). Cyclic di-GMP: the first 25 years of a universal bacterial second messenger. Microbiol Mol Biol Rev 77, 1-52.
Sauer, K., Cullen, M.C., Rickard, A.H., Zeef, L.A., Davies, D.G., and Gilbert, P. (2004). Characterization of nutrient-induced dispersion in Pseudomonas aeruginosa PAO1 biofilm. J Bacteriol 186, 7312-7326.
Schreiber, K., Boes, N., Eschbach, M., Jaensch, L., Wehland, J., Bjarnsholt, T., Givskov, M., Hentzer, M., and Schobert, M. (2006). Anaerobic survival of Pseudomonas aeruginosa by pyruvate fermentation requires an Usp-type stress protein. J Bacteriol 188, 659-668.
Sengupta, A., Sasikala, W.D., Mukherjee, A., and Hazra, P. (2012). Comparative study of flavins binding with human serum albumin: a fluorometric, thermodynamic, and molecular dynamics approach. Chemphyschem 13, 2142-2153.
Seshasayee, A.S., Fraser, G.M., and Luscombe, N.M. (2010). Comparative genomics of cyclic-di-GMP signalling in bacteria: post-translational regulation and catalytic activity. Nucleic Acids Res 38, 5970-5981.
Shu, C., Yi, G., Watts, T., Kao, C.C., and Li, P. (2012). Structure of STING bound to cyclic di-GMP reveals the mechanism of cyclic dinucleotide recognition by the immune system. Nat Struct Mol Biol 19, 722-724.
Sifri, C.D. (2008). Healthcare epidemiology: quorum sensing: bacteria talk sense. Clin Infect Dis 47, 1070-1076.
Simm, R., Morr, M., Kader, A., Nimtz, M., and Römling, U. (2004). GGDEF and EAL domains inversely regulate cyclic di-GMP levels and transition from sessility to motility. Mol Microbiol 53, 1123-1134.
Sintim, H.O., Smith, J.A., Wang, J., Nakayama, S., and Yan, L. (2010). Paradigm shift in discovering next-generation anti-infective agents: targeting quorum sensing, c-di-GMP signaling and biofilm formation in bacteria with small molecules. Future Med Chem 2, 1005-1035.
Son, M.S., Matthews, W.J., Kang, Y., Nguyen, D.T., and Hoang, T.T. (2007). In vivo evidence of Pseudomonas aeruginosa nutrient acquisition and pathogenesis in the lungs of cystic fibrosis patients. Infect Immun 75, 5313-5324.

Sperber, A.M., and Herman, J.K. (2017). Metabolism Shapes the Cell. J Bacteriol 199.
Srivastava, D., and Waters, C.M. (2012). A tangled web: regulatory connections between quorum sensing and cyclic Di-GMP. J Bacteriol 194, 4485-4493.
Stelitano, V., Brandt, A., Fernicola, S., Franceschini, S., Giardina, G., Pica, A., Rinaldo, S., Sica, F., and Cutruzzolà, F. (2013). Probing the activity of diguanylate cyclases and c-di-GMP phosphodiesterases in real-time by CD spectroscopy. Nucleic Acids Res 41, e79.
Stelitano, V., Giardina, G., Paiardini, A., Castiglione, N., Cutruzzolà, F., and Rinaldo, S. (2013). C-di-GMP hydrolysis by Pseudomonas aeruginosa HD-GYP phosphodiesterases: analysis of the reaction mechanism and novel roles for pGpG. PLoS One 8, e74920.
Taylor, B.L., and Zhulin, I.B. (1999). PAS domains: internal sensors of oxygen, redox potential, and light. Microbiol Mol Biol Rev 63, 479-506.
Tolker-Nielsen, T. (2014). Pseudomonas aeruginosa biofilm infections: from molecular biofilm biology to new treatment possibilities. APMIS Suppl, 1-51.
Valentini, M., and Filloux, A. (2016). Biofilms and Cyclic di-GMP (c-di-GMP) Signaling: Lessons from Pseudomonas aeruginosa and Other Bacteria. J Biol Chem 291, 12547-12555.
Wang, Y., Hay, I.D., Rehman, Z.U., and Rehm, B.H. (2015). Membrane-anchored MucR mediates nitrate-dependent regulation of alginate production in Pseudomonas aeruginosa. Appl Microbiol Biotechnol 99, 7253-7265.
Wassmann, P., Chan, C., Paul, R., Beck, A., Heerklotz, H., Jenal, U., and Schirmer, T. (2007). Structure of BeF3- -modified response regulator PleD: implications for diguanylate cyclase activation, catalysis, and feedback inhibition. Structure 15, 915-927.
Watnick, P., and Kolter, R. (2000). Biofilm, city of microbes. J Bacteriol 182, 2675-2679.
Weinhouse, H., Sapir, S., Amikam, D., Shilo, Y., Volman, G., Ohana, P., and Benziman, M. (1997). c-di-GMP-binding protein, a new factor regulating cellulose synthesis in Acetobacter xylinum. FEBS Lett 416, 207-211.
Wolfmeier, H., Pletzer, D., Mansour, S.C., and Hancock, R.E.W. (2018). New Perspectives in Biofilm Eradication. ACS Infect Dis 4, 93-106.

Annexes

Mantoni, F.*, Paiardini, A.*, Brunotti, P.*, D'Angelo, C., Cervoni, L., Paone, A., Cappellacci, L., Petrelli, R., Ricciutelli, M., Leoni, L., et al. (2018). Insights into the GTP-dependent allosteric control of c-di-GMP hydrolysis from the crystal structure of PA0575 protein from Pseudomonas aeruginosa. FEBS Journal doi:10.1111/febs.14634.

Paiardini, A.*, **Mantoni, F.***, Giardina, G., Paone, A., Janson, G., Leoni, L., Rampioni, G., Cutruzzolà, F., and Rinaldo, S. (2018). A novel bacterial L-arginine sensor controlling c-di-GMP levels in Pseudomonas aeruginosa. Proteins. doi:10.1002/prot.25587

Rinaldo, S., Giardina, G., **Mantoni, F.**, Paone, A., and Cutruzzolà, F. (2018). Beyond nitrogen metabolism: nitric oxide, cyclic-di-GMP and bacterial biofilms. FEMS Microbiol Lett 365.

Rinaldo, S., Giardina, G., **Mantoni, F.**, Paiardini, A., Paone, A., and Cutruzzolà, F. (2017). Discovering Selective Diguanylate Cyclase Inhibitors: From PleD to Discrimination of the Active Site of Cyclic-di-GMP Phosphodiesterases. Methods Mol Biol 1657, 431-453.

Di Salvio, M., Piccinni, V., Gerbino, V., **Mantoni, F.**, Camerini, S., Lenzi, J., Rosa, A., Chellini, L., Loreni, F., Carrì, M.T., et al. (2015). Pur-alpha functionally interacts with FUS carrying ALS-associated mutations. Cell Death Dis 6, e1943.

* These authors contributed equally to the correspondent works

Acknowledgements

The experimental data described in this PhD thesis was obtained at the Department of Biochemical Sciences 'Rossi Fanelli' of 'La Sapienza' University of Rome. Thanks to the passion and inspiration of many people, I was able to reach this important goal.
First of all, I want to thank my supervisor, Professor Cutruzzolà, for welcoming me in her Laboratory allowing me to begin this experience during which I had the opportunity to achieve many important goals.
A special thank to my tutor, Professor Rinaldo, for teaching me with passion and with (a lot of) patience.
A great thank to Dr. Giardina for his scientific advices and deep life tips.
A general, but not for this less felt, thank to all people daily working in Macromolecular Interaction and Mechanism Lab for making my working experience so pleasurable for these past three years.
Finally, a heartfelt thank to my great family, my girlfriend Francesca and my life-shared friends for supporting and for bearing me during this travel.